Opschoor, Daan; van der Wel, Michel

Working Paper

A Smooth Shadow-Rate Dynamic Nelson-Siegel Model for Yields at the Zero Lower Bound

Tinbergen Institute Discussion Paper, No. TI 2022-011/III

Provided in Cooperation with:
Tinbergen Institute, Amsterdam and Rotterdam

Suggested Citation: Opschoor, Daan; van der Wel, Michel (2022) : A Smooth Shadow-Rate Dynamic Nelson-Siegel Model for Yields at the Zero Lower Bound, Tinbergen Institute Discussion Paper, No. TI 2022-011/III, Tinbergen Institute, Amsterdam and Rotterdam

This Version is available at:
https://hdl.handle.net/10419/263931

TI 2022-011/III
Tinbergen Institute Discussion Paper

A Smooth Shadow-Rate Dynamic Nelson-Siegel Model for Yields at the Zero Lower Bound

Daan Opschoor[1,2]
Michel van der Wel[1,2]

1 Erasmus University Rotterdam

2 Tinbergen Institute

A Smooth Shadow-Rate Dynamic Nelson-Siegel Model for Yields at the Zero Lower Bound*

Daan Opschoor† Michel van der Wel

Econometric Institute, Erasmus University Rotterdam

January 27, 2022

Abstract

We propose a smooth shadow-rate version of the dynamic Nelson-Siegel (DNS) model to analyze the term structure of interest rates during the recent zero lower bound (ZLB) period. By relaxing the no-arbitrage restriction, our shadow-rate model becomes highly tractable with a closed-form yield curve expression. The model easily permits the implementation of readily available DNS extensions such as time-varying loadings, integration of macroeconomic variables and time-varying volatility. Using U.S. Treasury data, we provide clear evidence of a smooth transition of the yields entering and leaving the ZLB state. Moreover, we show that the smooth shadow-rate DNS model dominates the baseline DNS model in terms of fitting and forecasting the yield curve, while being competitive with a shadow-rate affine term structure model.

Keywords: Yield curve, zero lower bound, shadow-rate model, Nelson–Siegel curve

JEL Classification: E43, E47, C53, C58, G12

*We thank Robin Lumsdaine and Dick van Dijk for their helpful comments and discussions, as well as participants at the 15th International Conference on Computational and Financial Econometrics (CFE) (2021) and seminar participants at Erasmus University Rotterdam (2021).

†Corresponding author. Email addresses: opschoor@ese.eur.nl (Daan Opschoor), vanderwel@ese.eur.nl (Michel van der Wel).

1 Introduction

Accurately modelling and forecasting the term structure of interest rates is of key importance to market participants and financial institutions in the context of portfolio and risk management, derivatives pricing, and monetary policy. However, in the aftermath of the global financial crisis and the recent coronavirus pandemic, this task has become more challenging in several major economies due to a prolonged period of low interest rates close to the so-called zero lower bound (ZLB). This ZLB is an absorbing state and forces short-term yields to become flat and less volatile leading to asymmetric behaviour in the entire yield curve. Unfortunately, traditional term structure models are not able to capture these changed dynamics at the ZLB (see the discussions in Christensen and Rudebusch, 2015, 2016; Bauer and Rudebusch, 2016; Ullah, 2019, among others). As a result, there is a need for the development of tractable models that are able to handle the non-linearity of the term structure of interest rates at the ZLB.

To address this issue, we propose a smooth shadow-rate version of the dynamic Nelson-Siegel (DNS) model of Diebold and Li (2006) that softly imposes the ZLB onto the yields via the shadow short-rate concept of Black (1995). Our model is highly tractable and, in contrast to the no-arbitrage shadow-rate affine term structure models that we discuss below, neither needs computationally intensive numerical methods nor forward-rate data to be estimated. In addition, our modelling approach explicitly allows for a more gradual transition into and out of the ZLB state such that medium- and long-term yields, that are themselves not directly restricted by the ZLB, still recognize and account for the presence of a lower bound and its accompanying bounded short-term yields. The smooth shadow-rate DNS model also easily permits the implementation of readily available DNS model extensions, which we illustrate by allowing for time-varying factor loadings in the manner of Koopman et al. (2010) in order to capture further changed dynamics of the yield curve at the ZLB.

We consider monthly U.S. zero-coupon government bond yields from September 1981 to October 2020, which experienced a prolonged period of being subject to the ZLB from November 2008 to December 2015 and from March 2020 onwards.[1] Moreover, we put the smooth shadow-rate DNS model in a nonlinear state-space form such that it

[1]The sample starts in September 1981 as the three- and six-month yields are only available from this month onwards.

can be estimated with maximum likelihood estimation and extended Kalman filtering methods, see Durbin and Koopman (2012).[2] Our empirical analysis shows that our smooth shadow-rate DNS model provides a better in-sample fit than the DNS model in terms of log-likelihood value, information criteria and root mean squared errors (RMSE), especially during the ZLB period. In fact, the overall improvement in RMSE is about 8.5% over the total period and 38.8% over the ZLB period. Based on our estimated model, we also find evidence that there is a smooth transition from a high interest-rate to a low interest-rate environment, indicated by a significant smoothness parameter, which captures the gradual transition, as well as better fitting performance of the smooth shadow-rate model relative to a non-smooth version. This implies that the complete term structure of interest rates gradually enters and leaves the ZLB state. Furthermore, we provide evidence of time-varying loadings, where allowing for this feature in the DNS and smooth shadow-rate DNS seems to improve the in-sample fit even further. Finally, our smooth shadow-rate model produces a similar in-sample fit as the shadow-rate affine term structure model.

Next, we show that the original DNS model is not able to generate plausible future yield curve paths at the ZLB. Specifically, the DNS model lacks the ability to account for the compression of yield volatility at the ZLB, leading to improbably high positive probabilities of negative projected short- and medium-term yields. Meanwhile, the smooth shadow-rate DNS model imposes yields to be non-negative and therefore accurately replicates the low yield volatility at the ZLB. Our model additionally delivers valuable output that can be useful for shaping policy expectations. For example, we estimate liftoff horizons that indicate when the policy rate starts to diverge from the ZLB again, and find that these are close to the realized liftoff date in December 2015. Furthermore, we examine its shadow short-rate estimates and compare them to the measures of Wu and Xia (2016) and Krippner (2015a). Our estimates closely resemble these alternatives in terms of level and dynamics, but they are also sensitive to the specification of the lower bound value and smoothness parameter that governs the softness of the ZLB imposition. Yet, the sensitivity of shadow short rates estimates to specific modelling choices is also found in Christensen and Rudebusch (2015, 2016) and Krippner (2020), hence these estimates

[2]Alternatively, our smooth shadow-rate DNS model could be estimated with the two-step approach of Diebold and Li (2006) based on (nonlinear) least squares to make estimation even more tractable. Yet, this two-step procedure ignores the estimation uncertainty associated with the first step such that we instead opt for the one-step extended Kalman filter approach.

should always be used with caution.

Lastly, we assess the relative out-of-sample performance of the smooth shadow-rate DNS model. Most prominently, we find that our smooth shadow-rate DNS model outperforms the baseline DNS model for all forecasting horizons and yield horizons, where this improvement is strongest for longer horizons during the ZLB period. In contrast, the imposition of time-varying loadings does not lead to forecast improvements compared to constant loading models. We additionally find that our smooth shadow-rate model produces better forecasts than the shadow-rate affine term structure model for longer horizons and short-term yields, but is outperformed for long-term yields.

Our work is closely related to and builds on two strands of term structure modelling literature. First, it relates to the existing literature on shadow-rate term structure models that respect the ZLB.[3] Specifically, shadow-rate models impose that the observed short rate is the maximum of a lower bound, often assumed zero, and a shadow short-rate that would prevail in a world without physical currency and hence can become negative. Most, if not all, literature on shadow-rate models apply this concept in the framework of the theoretically consistent class of (no-arbitrage) affine term structure models (ATSM) (Vasicek, 1977; Cox et al., 1985; Duffie and Kan, 1996; Dai and Singleton, 2000). However, this implementation does not lead to closed-form analytic bond price formulas such that numerical methods (Gorovoi and Linetsky, 2004; Bomfim, 2003; Kim and Singleton, 2012; Ichiue and Ueno, 2007) or ZLB bond price approximations (Krippner, 2012; Christensen and Rudebusch, 2015, 2016; Wu and Xia, 2016; Bauer and Rudebusch, 2016) are required. Despite these advances, shadow-rate ATSM estimation remains computationally intensive (Bauer and Rudebusch, 2016), especially with a large number of parameters as in macro-finance models. Hence, we contribute to this strand of literature by providing a reduced-form shadow-rate model that is highly tractable, even in a large dimensional parameter space. This tractability comes at the cost of not necessarily satisfying the no-arbitrage restriction. Whether or not that matters a lot is an open question, as literature generally finds mixed results on the empirical importance of no-arbitrage restrictions and empirical difference of the DNS model and arbitrage-free models (see, for example, Duffee, 2011;

[3]Other term structure models that obey the ZLB are, among others, quadratic models (Kim and Singleton, 2012; Chung and Iiboshi, 2015; Chung et al., 2017; Andreasen and Meldrum, 2019), autoregressive gamma zero models (Monfort et al., 2017; Roussellet, 2020), linear-rational models (Filipović et al., 2017) and regime switching models (Christensen, 2015).

Coroneo et al., 2011; Krippner, 2015b).[4]

Second, our work is related to the strand of literature that employs reduced-form models for the term structure of interest rates. Most prominently, the DNS model of Diebold and Li (2006) gained popularity due to its simplicity, stable estimation and good in-sample and out-of-sample performance. Moreover, the DNS model allows itself to be fairly easily augmented in various directions. Extensions include the integration of macroeconomic variables (Diebold et al., 2006; Exterkate et al., 2013; Koopman and van der Wel, 2013; Coroneo et al., 2016), or adding time-varying volatility or factor loadings (Koopman et al., 2010; Caldeira et al., 2010; Laurini and Hotta, 2010; Hautsch and Ou, 2012; Hautsch and Yang, 2012; Hevia et al., 2015; Laurini and Caldeira, 2016), time-varying unconditional means (Dijk et al., 2014), or time-varying parameter vector autoregressions (Byrne et al., 2017). However, applying the reduced-form DNS model in the context of shadow-rate term structure modelling has, to the best of our knowledge, not been considered.[5] Our work bridges the gap between the shadow-rate class and reduced-form class of term structure models to obtain a model that obeys the ZLB and at the same time remains highly tractable. Besides the tractability, our novel shadow-rate DNS model thus has as appealing feature that there is the flexibility to incorporate the aforementioned model extensions.

The remainder of this paper is as follows. Section 2 introduces our smooth shadow-rate version of the DNS model. Section 3 discusses and presents the U.S. government bond yield data. Section 4 displays our empirical analysis in terms of in-sample and out-of-sample performance as well as some policy insights at the ZLB. Section 5 summarizes our main conclusions.

2 Smooth shadow-rate dynamic Nelson-Siegel model

In this section we discuss the dynamic Nelson-Siegel model of Diebold and Li (2006) and its augmentation into the smooth shadow-rate version that respects the ZLB. Moreover, we discuss the time-varying factor loading extension and the estimation framework of the

[4]For further discussion on and comparison of the DNS and arbitrage-free Nelson-Siegel (AFNS) models, see Diebold and Rudebusch (2013).

[5]Related work of Kang (2015) and Abdymomunov et al. (2016) does impose a ZLB restriction onto the DNS model, but this essentially boils down to a Bayesian estimation approach that restricts yields to be non-negative and does not reflect the idea of the shadow-rate framework.

models in a (non)linear state-space form.

2.1 Dynamic Nelson-Siegel model

The term structure of interest rates can take on a variety of shapes such as monotonically increasing or decreasing, humped and inverted humped. A parsimonious yield curve expression that is able to capture all these different shapes is the function proposed by Nelson and Siegel (1987). This function is, in turn, modified by Diebold and Li (2006) to allow for time-varying factors resulting in the expression

$$y_t(\tau) = \beta_{1t} + \beta_{2t}\left(\frac{1-e^{-\lambda\tau}}{\lambda\tau}\right) + \beta_{3t}\left(\frac{1-e^{-\lambda\tau}}{\lambda\tau} - e^{-\lambda\tau}\right), \tag{1}$$

where $y_t(\tau)$ is the yield of a zero-coupon bond at time t with time to maturity τ, λ is the factor loading parameter, and β_{1t}, β_{2t} and β_{3t} are latent time-varying factors, which have the interpretation of level, slope and curvature, respectively.

These factor interpretations are explicitly imposed by the factor loading structure. More specifically, the level factor is a long-term factor as it has a constant loading that does not decay to zero when time to maturity increases, that is, $\lim_{\tau\to\infty} y_t(\tau) = \beta_{1t}$. The slope factor is a short-term factor as its loading starts at one and converges to zero when time to maturity increases, while the curvature factor is a medium-term factor as its loading start at zero, then increases, but in the end converges to zero when time to maturity increases. Lastly, the model-implied short rate r_t is given by the sum of the level and slope factors, that is, $r_t = \lim_{\tau\to 0} y_t(\tau) = \beta_{1t} + \beta_{2t}$.

The model lends itself to be easily written in state space form, following Diebold et al. (2006). Given a set of N observed yields at time t, collected in the observation vector $\boldsymbol{y}_t^o = (y_t^o(\tau_1), \ldots, y_t^o(\tau_N))'$, the measurement equation is given by

$$\boldsymbol{y}_t^o = \boldsymbol{\Lambda}(\lambda)\boldsymbol{\beta}_t + \boldsymbol{\varepsilon}_t, \qquad \boldsymbol{\varepsilon}_t \sim \mathcal{N}(\mathbf{0}, \boldsymbol{\Sigma}_\varepsilon), \tag{2}$$

for $t = 1, \ldots, T$, where $\boldsymbol{\beta}_t = (\beta_{1t}, \beta_{2t}, \beta_{3t})'$ is the 3×1 vector with latent factors, $\boldsymbol{\varepsilon}_t$ is the $N \times 1$ measurement disturbance vector with covariance matrix $\boldsymbol{\Sigma}_\varepsilon$, and $\boldsymbol{\Lambda}(\lambda)$ is the

$N \times 3$ factor loading matrix given by

$$\boldsymbol{\Lambda}(\lambda) = \begin{pmatrix} 1 & \frac{1-\mathrm{e}^{-\lambda\tau_1}}{\lambda\tau_1} & \frac{1-\mathrm{e}^{-\lambda\tau_1}}{\lambda\tau_1} - e^{-\lambda\tau_1} \\ \vdots & \vdots & \vdots \\ 1 & \frac{1-\mathrm{e}^{-\lambda\tau_N}}{\lambda\tau_N} & \frac{1-\mathrm{e}^{-\lambda\tau_N}}{\lambda\tau_N} - e^{-\lambda\tau_N} \end{pmatrix}.$$

Furthermore, we model the dynamics of $\boldsymbol{\beta}_t$ as a vector autoregressive (VAR) process of order 1 such that the state equation is given by

$$\boldsymbol{\beta}_t = \boldsymbol{\alpha} + \boldsymbol{\Gamma}\boldsymbol{\beta}_{t-1} + \boldsymbol{\eta}_t, \qquad \boldsymbol{\eta}_t \sim \mathcal{N}(\mathbf{0}, \boldsymbol{\Sigma}_\eta), \tag{3}$$

for $t = 1, \ldots, T$, where $\boldsymbol{\alpha}$ is a 3×1 vector with constants, $\boldsymbol{\Gamma}$ is a 3×3 matrix with VAR coefficients and $\boldsymbol{\eta}_t$ is the 3×1 state disturbance vector with covariance matrix $\boldsymbol{\Sigma}_\eta$. The initial conditions are specified as $\boldsymbol{\beta}_0 \sim \mathcal{N}(\boldsymbol{\mu}, \boldsymbol{\Sigma}_\beta)$, where $\boldsymbol{\mu} = (\boldsymbol{I} - \boldsymbol{\Gamma})^{-1}\boldsymbol{\alpha}$ and covariance matrix $\boldsymbol{\Sigma}_\beta$ is chosen such that it satisfies $\boldsymbol{\Sigma}_\beta - \boldsymbol{\Gamma}\boldsymbol{\Sigma}_\beta\boldsymbol{\Gamma}' = \boldsymbol{\Sigma}_\eta$, see Hamilton (1994, section 2.2) for further details. We ensure stationarity of the VAR process via the reparameterization of $\boldsymbol{\Gamma}$ and $\boldsymbol{\Sigma}_\eta$ as proposed by Ansley and Kohn (1986). Moreover, we follow Diebold et al. (2006) and assume for computational tractability that $\boldsymbol{\Sigma}_\varepsilon$ is diagonal, while $\boldsymbol{\Sigma}_\eta$ remains non-diagonal. The complete dynamic Nelson-Siegel (DNS) model is given by equations (2) and (3).

2.2 Imposing a smooth lower-bound restriction

On its own, the DNS model does not restrict yields to be non-negative and, consequently, assumes that the yield curve behaves the same in low interest-rate environments as in high interest-rate environments. However, Black (1995) already notes that the observed short rate in the market cannot become (too) negative due to the presence of a physical currency with a natural interest rate of zero.[6] Therefore, the short rate r_t is the maximum of a lower bound r_{LB} and a shadow short rate s_t that would prevail in a world without the option of physical currency, that is, $r_t = \max(r_{LB}, s_t)$.

By assuming that all yields can not go below the lower bound value, we generalize

[6] In practice, the natural interest rate of physical currency is not exactly zero due to transaction and storage costs.

this idea directly onto the yield curve such that

$$\underline{y}_t(\tau) = r_{LB} + \max\Big(0, y_t(\tau) - r_{LB}\Big),$$

where $\underline{y}_t(\tau)$ is called the zero lower bound (ZLB) yield curve and $y_t(\tau)$ is now called the shadow yield curve.[7] Plugging in the Nelson-Siegel equation (1) as shadow yield curve, results in a DNS model that imposes yields to be equal or larger than the lower bound r_{LB} and for which the shadow short rate is equal to $s_t = \beta_{1t} + \beta_{2t}$. We refer to this model as the shadow-rate DNS (B-DNS) model.[8]

This direct lower bound approach nevertheless assumes that yields are either behaving in a traditional way above r_{LB} or are flat and equal to r_{LB}. That is, the B-DNS model is non-smooth with a kink at r_{LB} that separates yields into two possible states. Consequently, an interest rate close, but above, the lower bound value (say, 0.25%) behaves similarly as when it is further away from the lower bound (say, 4%), while it seems more plausible that the asymmetry of the ZLB already starts to present at small, but positive, interest-rate levels close to the lower bound (say at 1%). This is particularly relevant for medium- and longer-term yields that are themselves not directly constrained by the ZLB, but experience the asymmetry caused by the restricted short-term yields. Therefore, we introduce a smoother transition between a high interest-rate state and the ZLB state. To do so, we consider a smooth approximation function of the max function, denoted by $f(\cdot)$, such that we obtain the ZLB yield curve expression

$$\underline{y}_t(\tau) = r_{LB} + \gamma f\left(\frac{y_t(\tau) - r_{LB}}{\gamma}\right), \tag{4}$$

where $\gamma > 0$ measures the smoothness of the approximation. We adopt the function $f(x) = x\Phi(x) + \phi(x)$ that could be obtained as the antiderivative of $\Phi(\cdot)$, where $\Phi(\cdot)$ and $\phi(\cdot)$ are the cumulative and probability density functions of the standard normal distribution, respectively.[9] This specific function $f(\cdot)$ is inspired by the ZLB forward-rate

[7] Note that the assumption that all yields can not go below the lower bound value is also implicitly made in the shadow-rate affine term structure models, see the discussion in Christensen and Rudebusch (2015, p. 233).

[8] We follow the convention of Kim and Singleton (2012) to use the prefix "B-" for a shadow-rate model in the spirit of Black (1995).

[9] Naturally, there exist various other functions that could be used for this approximation such as the softplus function $f(x) = \log(1 + e^x)$. However, we opt for the function $f(x) = x\Phi(x) + \phi(x)$ due to its resemblance with the ZLB forward-rate approximation in the no-arbitrage shadow-rate models.

approximation of Krippner (2012) and Wu and Xia (2016) in the context of a shadow-rate affine term structure model.[10] The advantage of our reduced-form DNS framework is that we can directly impose the function onto the yield curve without the need for numerical integration, while in these aforementioned papers the ZLB forward-rate approximation does require numerical integration to obtain the ZLB yield curve.

Figure 1 shows the smooth approximation of the max function for a range of values of γ. From the figure it is clear that a higher (smaller) value of γ results in a less (more) noticeable kink. In the context of the ZLB forward rate approximation in the shadow-rate affine term structure model class, this smoothness parameter γ is related to the conditional variance in the shadow-bond option-price formula such that it becomes a function of the time-to-maturity and risk-neutral volatility parameters of the latent factor dynamics (Christensen and Rudebusch, 2015). However, in our reduced-form framework the parameter γ can be specified more freely. For example, we can pre-specify γ, say at a value of 1, or it can be estimated as a free parameter. In fact, γ could be specified as a function of the time-to-maturity τ, for example, by using spline functions, or even made time-varying, but these extensions are left for further research.[11]

Taking the function $f(x) = x\Phi(x) + \phi(x)$ and plugging it into equation (4) provides

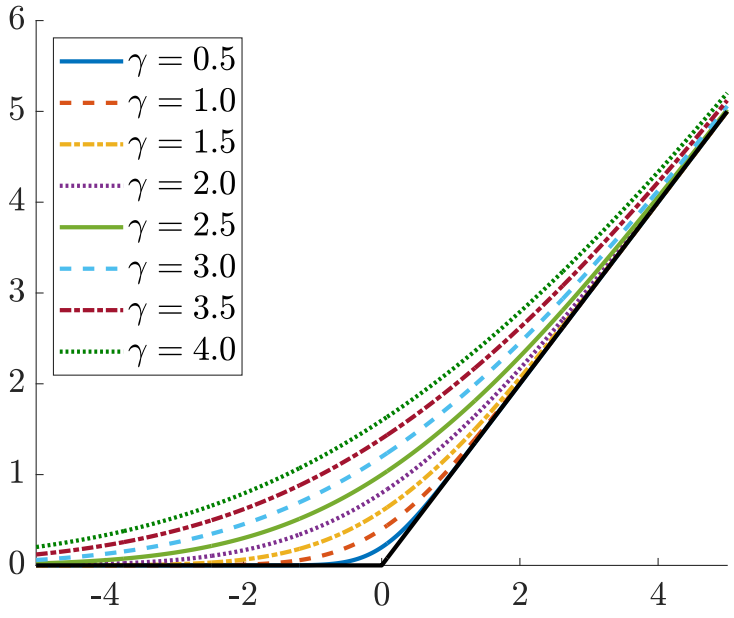

Figure 1: Illustration of the function $\gamma f(\cdot/\gamma)$ as approximation of the max function

[10] See Appendix A for further details on this approach in the context of the shadow-rate arbitrage-free Nelson-Siegel (B-AFNS) model of Christensen and Rudebusch (2015, 2016).

[11] Some preliminary results in Appendix B indeed show that the estimate of γ is slightly decreasing as a function of τ.

the smooth ZLB yield curve

$$\underline{y}_t(\tau) = r_{LB} + (y_t(\tau) - r_{LB})\Phi\left(\frac{y_t(\tau) - r_{LB}}{\gamma}\right) + \gamma\phi\left(\frac{y_t(\tau) - r_{LB}}{\gamma}\right).$$

We refer to this model as the smooth shadow-rate DNS (SB-DNS) model. Writing again $\boldsymbol{y}_t^o$ for the observation vector at time t, the measurement equation of the SB-DNS model is given by

$$\boldsymbol{y}_t^o = r_{LB}\boldsymbol{\iota} + (\boldsymbol{\Lambda}(\lambda)\boldsymbol{\beta}_t - r_{LB}\boldsymbol{\iota}) \odot \boldsymbol{F}_t + \gamma \boldsymbol{f}_t + \boldsymbol{\varepsilon}_t, \qquad \boldsymbol{\varepsilon}_t \sim \mathcal{N}(\boldsymbol{0}, \boldsymbol{\Sigma}_\varepsilon), \tag{5}$$

where $\odot$ is the Hadamard product, $\boldsymbol{\iota}$ denotes an $N \times 1$ vector with ones, $\boldsymbol{F}_t = (F_{1t}, \ldots, F_{Nt})'$ with $F_{it} = \Phi\big((y_t(\tau_i) - r_{LB})/\gamma\big)$ and $\boldsymbol{f}_t = (f_{1t}, \ldots, f_{Nt})'$ with $f_{it} = \phi\big((y_t(\tau_i) - r_{LB})/\gamma\big)$. We thus get a nonlinear state-space model as the factors $\boldsymbol{\beta}_t$ appear in the nonlinear functions $\Phi(\cdot)$ and $\phi(\cdot)$ in $\boldsymbol{F}_t$ and $\boldsymbol{f}_t$ of equation (5), as well as in $\boldsymbol{\Lambda}(\lambda)\boldsymbol{\beta}_t - r_{LB}\boldsymbol{\iota}$. The state equation of the SB-DNS model, governing the dynamics of the factors, is the same as for the DNS model in equation (3).

2.3 Time-varying factor loadings

To demonstrate the potential and model flexibility of the SB-DNS model to be easily augmented with readily available DNS extensions, we allow for time-varying factor loadings based on the approach of Koopman et al. (2010). Consequently, this enables us to examine whether time-varying loadings help to capture changed dynamics of the yield curve at the ZLB, as was suggested by Diebold and Rudebusch (2013, p. 103). This has, to the best of our knowledge, not been assessed yet. Traditionally, the DNS model assumes constant factor loadings via a time-invariant parameter λ, where Diebold and Li (2006) fix λ at 0.0609 such that it maximizes the curvature factor loading at a maturity of 30 months, while Diebold et al. (2006) estimate it to be 0.077 in a state-space framework with a maximum at 23.3 months. Meanwhile, the arbitrage-free Nelson-Siegel (AFNS) model of Christensen et al. (2011) and its shadow-rate counterpart (Christensen and Rudebusch, 2015) require λ to be constant over time in order to impose the no-arbitrage restriction.[12]

[12]Recently, though, Han et al. (2021) relax this strict assumption needed for the no-arbitrage restriction and generalize the AFNS model to have a time-varying loading, which they show to have predictive

Koopman et al. (2010) argue that the assumption of constant factor loadings might be too restrictive since the factor structure of the slope and curvature factors could change over time. Koopman et al. (2010) and Laurini and Caldeira (2016) indeed show that λ_t is time-varying for U.S. government bond yields and that incorporating this feature improves the fit relative to constant loadings, whereas this improvement is even more pronounced in emerging markets such as Brazil (Caldeira et al., 2010). To implement this feature into the baseline and smooth shadow-rate DNS models, we follow Koopman et al. (2010) and consider $\beta_{4t} = \lambda_t$ to be an additional latent factor such that the state equation (3) increases in dimension with a fourth latent factor. We denote the corresponding models as (SB-)DNS-TVL.

2.4 Estimation framework

The DNS model given by equations (2)-(3) falls in the class of linear Gaussian state-space models such that, given the parameter set Θ consisting of λ and the elements in $\boldsymbol{\alpha}$, $\boldsymbol{\Gamma}$, $\boldsymbol{\Sigma}_\varepsilon$ and $\boldsymbol{\Sigma}_\eta$, the latent factors in the state vector can be recursively estimated via the Kalman filter (KF). Furthermore, the SB-DNS model with measurement equation (5) and state equation (3) as well as the TVL models fall in the class of nonlinear Gaussian state-space models, with Θ potentially extended to include r_{LB} and γ, such that the latent factors can be estimated via the extended Kalman filter (EKF). For a complete treatment of the KF and EKF, see Durbin and Koopman (2012). Given the estimated/predicted states, we can evaluate the log-likelihood function based on the prediction error decomposition. We numerically maximize the log-likelihood function with respect to Θ via a quasi-Newton optimization method, where the starting values are obtained via the two-step estimation approach of Diebold and Li (2006). For further details on the estimation framework and the (E)KF recursions, see Appendix C.

3 Data

In our empirical application we consider U.S. Treasury zero-coupon bond yields for eight maturities, namely three months, six months, one year, two years, three years, five years, seven years and ten years, which are similar to the ones used by Christensen and Rude-

power for business cycles and real economic activity.

busch (2016). The yields are obtained from the H.15 series of the Federal Reserve Board, where we take the end-of-the-month yield observations, starting from the date where they become available for all maturities, that is, September 1981 up to October 2020, resulting in 470 monthly observations.[13]

Table 1 displays the summary statistics of the monthly yields across maturities containing the mean, standard deviation, minimum, maximum and three autocorrelations. The yield curve is on average upward sloping, which also holds for the minimum of the

Table 1: Summary statistics of U.S. government bond yields across maturities

	Maturities (in months)							
	3	**6**	**12**	**24**	**36**	**60**	**84**	**120**
Panel A: Total period (September 1981 - October 2020)								
Mean	3.89	4.07	4.24	4.58	4.79	5.15	5.43	5.63
Std.	3.21	3.32	3.39	3.48	3.46	3.34	3.25	3.14
Min.	0.00	0.03	0.09	0.11	0.11	0.21	0.39	0.55
Max	15.05	16.19	16.64	16.69	16.45	16.27	16.05	15.84
$\hat{\rho}(1)$	0.99	0.99	0.99	0.99	0.99	0.99	0.99	0.99
$\hat{\rho}(12)$	0.88	0.89	0.89	0.91	0.92	0.92	0.93	0.93
$\hat{\rho}(24)$	0.75	0.77	0.79	0.83	0.86	0.88	0.89	0.90
Panel B: Pre-ZLB period (September 1981 - October 2008)								
Mean	5.38	5.61	5.81	6.21	6.41	6.72	6.94	7.08
Std.	2.71	2.83	2.89	2.94	2.91	2.80	2.75	2.67
Min.	0.46	0.94	1.09	1.32	1.58	2.30	2.87	3.37
Max	15.05	16.19	16.64	16.69	16.45	16.27	16.05	15.84
$\hat{\rho}(1)$	0.99	0.99	0.99	0.99	0.99	0.99	0.99	0.99
$\hat{\rho}(12)$	0.77	0.78	0.80	0.82	0.83	0.85	0.86	0.87
$\hat{\rho}(24)$	0.56	0.58	0.63	0.70	0.74	0.79	0.82	0.84
Panel C: ZLB period (November 2008 - December 2015)								
Mean	0.08	0.16	0.26	0.55	0.86	1.52	2.07	2.56
Std.	0.06	0.10	0.16	0.27	0.39	0.54	0.62	0.63
Min.	0.00	0.03	0.09	0.20	0.30	0.59	0.98	1.51
Max	0.26	0.49	0.90	1.14	1.70	2.69	3.39	3.85
$\hat{\rho}(1)$	0.78	0.83	0.83	0.90	0.91	0.92	0.92	0.92
$\hat{\rho}(12)$	0.23	0.26	0.38	0.52	0.49	0.36	0.31	0.29
$\hat{\rho}(24)$	0.34	0.16	0.00	-0.26	-0.39	-0.39	-0.31	-0.17

Notes: This table contains the mean, standard deviation (std.), minimum (min.) and maximum (max.) of monthly U.S. government bond yields across maturities in percentage points. The rows with $\hat{\rho}(1)$, $\hat{\rho}(12)$, $\hat{\rho}(24)$ display the one month, one year and two year sample autocorrelations, respectively.

[13]The data set of the H.15 series can be found at https://www.federalreserve.gov/releases/h15/default.htm. Further details about the yield curve data methodology are available at https://home.treasury.gov/policy-issues/financing-the-government/interest-rate-statistics.

yields. Indeed, Figure 2 shows that long-term yields are generally above short-term yields. Next, we see that after the global financial crisis (GFC) of 2007-2008 short-term yields have been close to the ZLB for a prolonged period from December 2008 till December 2015. After this ZLB period, interest rates started to increase again until the corona virus pandemic hit, which brought yields back to the ZLB. The ZLB periods are indicated with grey in the figures.

The ZLB period is accompanied with changed dynamics for the entire yield curve. Table 1 shows summary statistics also for the pre-ZLB period (Panel B) and for the ZLB period (Panel C). During the pre-ZLB period there seems to be an inverted U-shape curve between the yield curve volatility (measured as the standard deviation) and the time to maturity, with the highest volatility at the two-year maturity. However, during the ZLB period there exists an increasing volatility pattern in maturity as short-term yields are stuck at the ZLB. This compression of the short-term yield level and volatility relative to long-term yields is also observed in Figure 2. Furthermore, Table 1 shows that yields are less persistent during the ZLB period than is observed during the pre-ZLB period. In particular, long-term yields are more persistent than short-term yields during the pre-ZLB period, whereas this stylized fact disappears for the one and two year autocorrelations during the ZLB period. Overall, these changes in dynamics indicate the need of a model that accounts for the yield asymmetry and volatility compression at the ZLB.

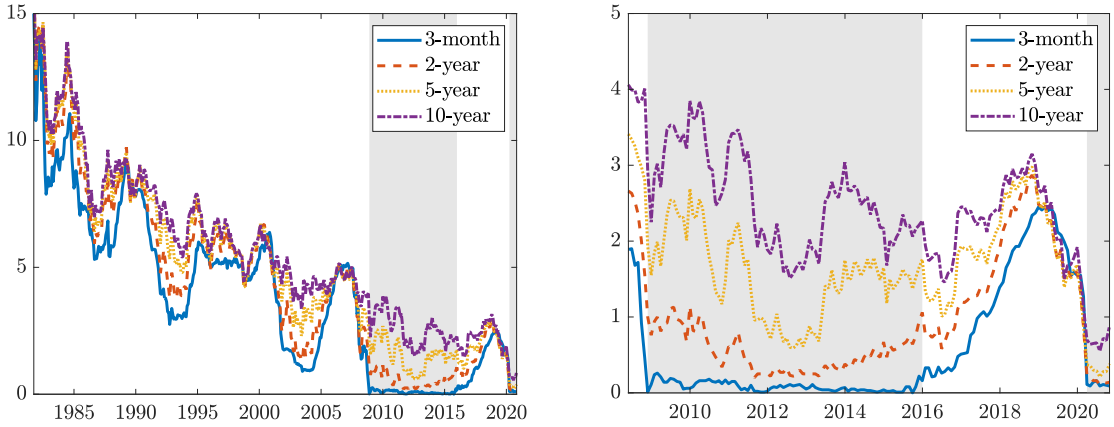

(a) Total period **(b)** Post-GFC period

Figure 2: Time series of U.S. government bond yields with shaded ZLB periods. Panel (a) shows the full sample-period while panel (b) zooms in on the period after the global financial crisis.

4 Empirical results

In Section 4.1 we first assess the estimation results and in-sample fit of the smooth shadow-rate model compared to the baseline DNS model, time-varying factor loading models and (shadow-rate) affine term structure models. Next, in Section 4.2 we examine the shortcomings of the DNS model at the ZLB and how these are resolved with the smooth shadow-rate adaption, after which we look in Section 4.3 how our novel model is able to provide policy insights during ZLB periods. Lastly, in Section 4.4 we examine the relative out-of-sample performance of the smooth shadow-rate model compared to other benchmarks.

4.1 In-sample fit

We start our in-sample fit analysis by comparing the estimated models in terms of their log-likelihood values, Akaike information criteria (AIC) and Bayesian information criteria (BIC), which are given in Table 2. Following the recommendation of Christensen and Rudebusch (2016) for U.S. government bond yields, we estimate all shadow-rate models with a fixed lower-bound specification of 0%, something which we relax in Appendix D.[14] The table presents the DNS and SB-DNS models with and without time-varying loadings (indicated with TVL in the table) and the B-DNS model. We also include the closest affine term structure model and its shadow-rate counterpart: the arbitrage-free Nelson-Siegel (AFNS) model of Christensen et al. (2011) and the shadow-rate AFNS model of Christensen and Rudebusch (2015), see Appendix A for further details.

There are three key findings based on this comparison. First, by comparing the DNS and SB-DNS model, we find that the imposition of the smooth shadow-rate framework results in a substantial gain in the log-likelihood value from 2615.7 to 3080.6. This gain is accompanied with only one additional free parameter that is estimated, namely the smoothness parameter γ. The AIC and BIC values indeed indicate that, despite the penalization of the additional model parameter, the SB-DNS model is still preferred over the baseline DNS model. The maximum likelihood estimate of γ is equal to 2.679 with a standard error of 0.206.[15] Hence, the estimate of γ is highly significant and provides

[14] For some regions, for example in Europe, it seems more plausible to have a time-varying lower bound, see Kortela (2016), Lemke and Vladu (2017) and Wu and Xia (2020), among others. This can easily be accommodated in our SB-DNS model as well, but these applications are left for further research.

[15] The complete overview of parameter estimates of the DNS and SB-DNS models are given in Ap-

Table 2: Log-likelihood values and information criteria

	Log-likelihood	**#Θ**	**AIC**	**BIC**	**LR-statistic**
DNS	2615.7	27	-11.0	-10.8	
DNS-TVL	3007.6	38	-12.6	-12.3	783.8
B-DNS	2614.1	27	-11.0	-10.8	X
SB-DNS	3080.6	28	-13.0	-12.7	929.8
SB-DNS-TVL	3251.0	39	-13.7	-13.3	1270.5
AFNS	2245.1	27	-9.4	-9.2	
B-AFNS	2593.2	27	-10.9	-10.7	

Notes: This table contains the log-likelihood values, Akaike information criteria (AIC), Bayesian information criteria (BIC) and the likelihood-ratio (LR) test statistics across models. The LR test statistics consider the DNS as null. We discard the first three observations from this calculation to make the results robust to the initial conditions. The shadow-rate models are estimated with a fixed lower-bound specification of $r_{LB} = 0\%$, while the smooth shadow-rate models have an estimated smoothness parameter γ.

strong evidence of a smooth transition into the ZLB state. Notably, the B-DNS model has a substantially lower log-likelihood value than the SB-DNS model. In fact, its log-likelihood value is even smaller than the one of the baseline DNS model, although the difference is small. The filtered yield factors of the DNS and SB-DNS models are shown and compared in Figure 3. The filtered factors of the DNS and SB-DNS models differ more for the slope and curvature factors than for the level factor, where for all factors the differences are more pronounced during the shaded ZLB periods. The differences between the filtered shadow short rate and short rate proxies the ZLB wedge measure, which gauges how tightly the ZLB restricts the yield curve, see for example Bauer and Rudebusch (2016) for a more detailed discussion on the ZLB wedge. As expected, this wedge is large during the ZLB period. However, it is also sizeable outside of this period, when yields are close to zero, as for example was the case during 2002 through 2005.

Second and consistent with the findings of Koopman et al. (2010), we find that allowing for time-varying factor loadings results in a significant improvement in the log-likelihood value for both the DNS and SB-DNS model with likelihood gains of 391.1 and 170.4, respectively. When introducing time-varying loadings, 11 new parameters are introduced, but penalizing the number of parameters still results in lower AIC and BIC values for the time-varying loading models. Figure 4 plots the filtered factor loading parameter. For both the DNS and SB-DNS variant with time-varying loadings the se-

pendix B.

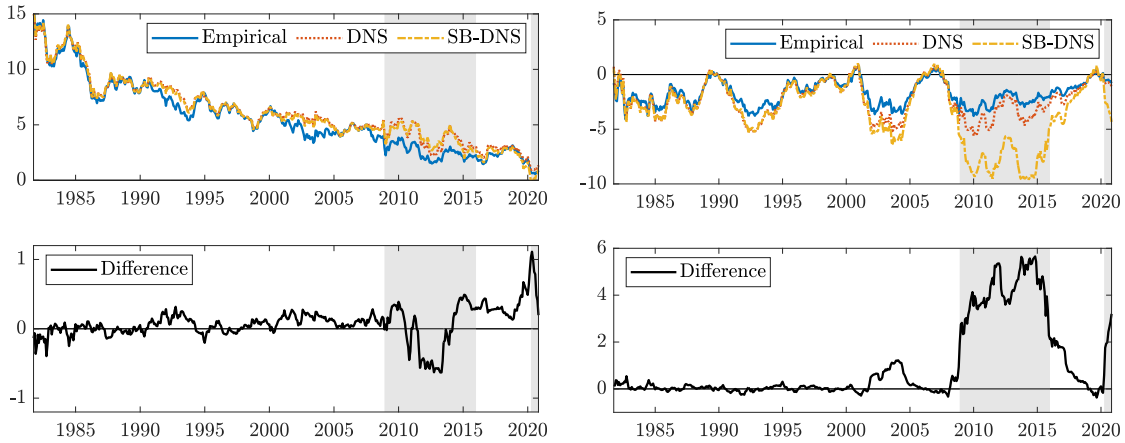

(a) Filtered level factors **(b)** Filtered slope factors

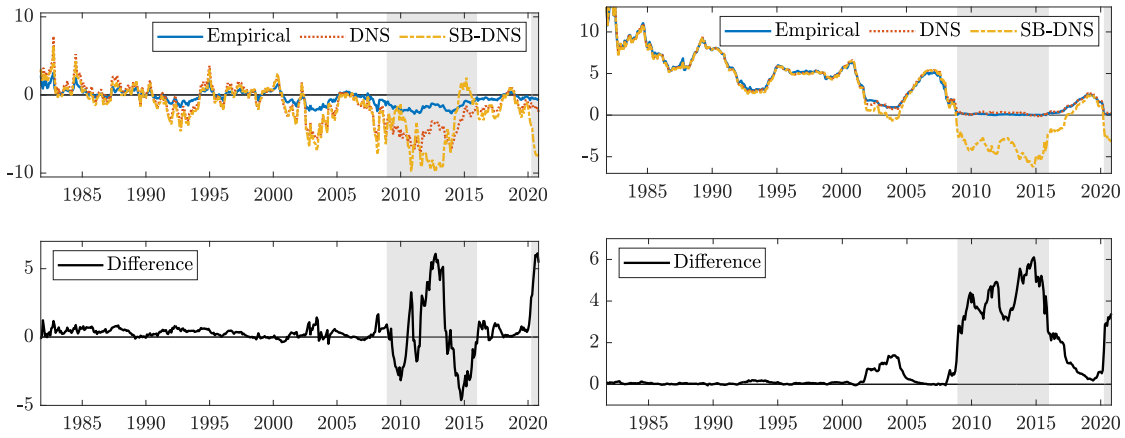

(c) Filtered curvature factors **(d)** Filtered (shadow) short rate

Figure 3: Filtered factors with their empirical proxies of the level (10-year yield), slope (3-month minus 10-year yield), curvature (twice the 2-year yield minus the sum of the 3-month and 10-year yields), and short rate (3-month yield) as well as the differences between the filtered factors of the DNS and SB-DNS models with shaded ZLB periods

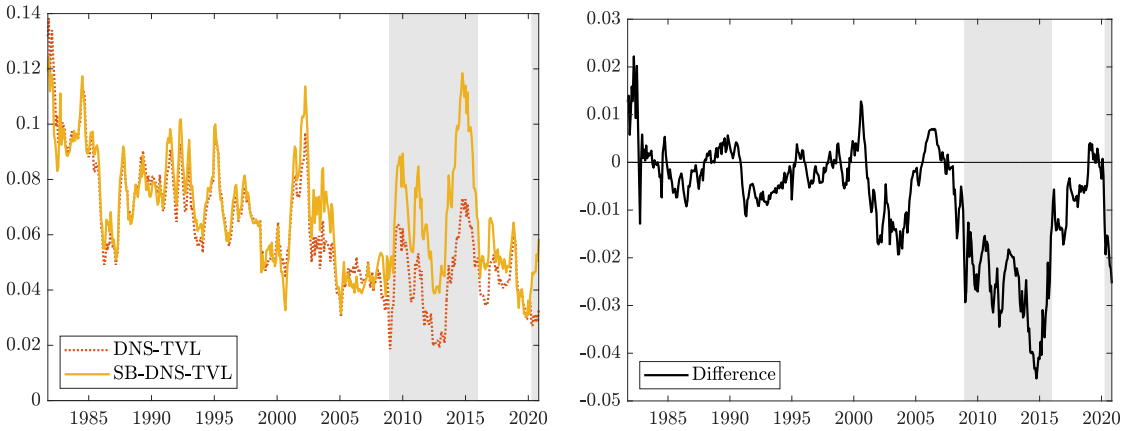

(a) Filtered TVLs **(b)** DNS-TVL minus SB-DNS-TVL

Figure 4: Filtered time-varying factor loading parameters of the DNS-TVL and SB-DNS-TVL models and their differences with shaded ZLB periods

ries behave similarly and both display strong time-variation. The loadings differ most strongly during the ZLB period, albeit also outside of it, where they are slightly higher for the SB-DNS model during the ZLB periods than for the DNS model.

Third, when comparing with the AFNS and B-AFNS models, there is a stark difference in likelihood. The log-likelihood values of the (B-)AFNS model variants are substantially lower than the ones of the DNS and SB-DNS model. Nevertheless, also for the AFNS model class it is clear that the imposition of the shadow-rate framework improves the log-likelihood value and information criteria.

Next, we assess the in-sample fit across models in terms of their root mean squared errors (RMSEs). Table 3 presents the RMSEs of the aforementioned models for all eight maturities during the total sample period, the pre-ZLB period and the ZLB period. For all three periods, the SB-DNS model has a lower RMSE than the DNS model for five out of eight maturities, where the DNS model seems to overfit the three-month and three-year yields.[16] Figure 5 presents the yield curve fit for nine selected dates, with varying yield curve shapes. Both the DNS and SB-DNS model are able to accurately fit the different yield curve shapes, although the SB-DNS model seems to be more flexible for short- and long-term yields. Specifically, on 27 February 2004, which occurs during the low interest rate period of 2004, the DNS and SB-DNS model have a highly similar yield curve fit for all maturities. This also holds for 31 December 2008, just after the FOMC announcement of cutting the federal funds rate for the first time to the 0%-0.25% range.[17] However, the dates occurring in the middle of a ZLB period (that is, 29 October 2010, 31 August 2011 and 30 October 2020) clearly show a better fit of the SB-DNS model, particularly for short-term maturities. The overall improvement across maturities in RMSE of the SB-DNS model relative to the DNS model is about 8.5% for the total period, 6.7% for the pre-ZLB period, and 38.3% for the ZLB period. Noteworthy, the B-DNS model has a similar in-sample fit as the DNS model, which indicates that the imposition of the smooth lower bound restriction really helps to improve the fit relative to a hard lower bound. To summarize, the SB-DNS model delivers a substantial improvement in terms of in-sample fit relative to the DNS and B-DNS models, particularly during the ZLB period.

The inclusion of time-varying factor loadings improves the total RMSE relative to the

[16]This overfitting seems to be an idiosyncrasy of this selection of maturities as Christensen and Rudebusch (2016) find something similar for the AFNS model and the one-year and three-year yields.

[17]See the FOMC statement on 16 December 2008: https://www.federalreserve.gov/newsevents/pressreleases/monetary20081216b.htm.

Table 3: In-sample model fit

RMSE	**Maturities (in months)**								**Total**
	3	**6**	**12**	**24**	**36**	**60**	**84**	**120**	
Panel A: Total period (December 1981 - October 2020)									
DNS	18.1	**0.0**	8.8	6.8	**0.0**	5.6	**3.0**	7.1	8.2
DNS-TVL	**14.1**	2.2	6.2	**4.9**	1.8	**4.6**	4.8	2.5	**6.3**
B-DNS	18.1	0.0	8.7	6.8	0.0	5.6	3.0	7.0	8.2
SB-DNS	17.4	1.7	7.5	5.1	1.6	5.0	4.1	3.8	7.5
SB-DNS-TVL	15.6	2.3	**6.2**	4.9	2.2	4.7	4.6	**2.4**	6.8
AFNS	16.7	2.1	8.1	5.3	0.1	6.1	4.2	7.5	7.8
B-AFNS	16.0	1.8	8.4	5.0	1.5	5.7	4.0	6.3	7.5
Panel B: Pre-ZLB period (December 1981 - October 2008)									
DNS	20.7	**0.0**	9.2	6.8	**0.0**	5.8	**3.0**	6.3	9.0
DNS-TVL	**16.1**	2.5	**6.8**	**5.5**	1.8	**5.1**	4.9	2.6	**7.1**
B-DNS	20.7	0.0	9.2	6.8	0.0	5.8	3.1	6.3	9.0
SB-DNS	20.0	1.0	8.3	5.7	1.4	5.2	4.3	3.9	8.4
SB-DNS-TVL	17.8	1.8	6.8	5.6	2.1	5.2	4.9	**2.4**	7.6
AFNS	19.3	2.3	9.0	5.5	0.1	6.4	4.1	7.1	8.6
B-AFNS	18.6	1.4	9.7	5.6	1.2	6.2	3.8	6.4	8.4
Panel C: ZLB period (November 2008 - December 2015)									
DNS	11.0	**0.0**	8.8	7.9	**0.0**	5.9	**3.3**	10.7	7.3
DNS-TVL	7.5	1.1	4.9	3.3	2.0	3.7	5.3	**2.9**	4.3
B-DNS	10.9	0.0	8.6	7.9	0.0	5.9	3.4	10.7	7.2
SB-DNS	8.1	2.1	4.4	3.4	2.0	4.6	4.4	4.1	4.5
SB-DNS-TVL	8.0	2.6	**3.6**	**2.5**	2.3	**3.4**	4.5	2.9	**4.1**
AFNS	9.5	1.8	6.6	5.9	0.1	6.5	5.1	10.2	6.6
B-AFNS	**7.2**	2.4	4.5	3.3	2.0	4.7	4.7	6.6	4.8

Notes: This table contains the Root Mean Squared Errors (RMSE) in basis points across maturities and baseline, time-varying loading and shadow-rate models over three sample periods. We discard the first three observations from this calculation to make the results robust to the initial conditions. The shadow-rate models are all estimated with a fixed lower bound specification of $r_{LB} = 0\%$, while the smooth shadow-rate models have an estimated smoothness parameter γ. The bold numbers indicate the lowest RMSE for that particular maturity and period.

baseline DNS model even further for all three periods. Specifically, the decrease in total RMSE is about 23.2% for the total period, 21.1% for the pre-ZLB period, and 41.1% for the ZLB period. Including time-varying factor loadings in the SB-DNS model also seems to improve the fit, albeit to a lesser extent, with decreases in total RMSE of 9.3% for the total period, 9.5% for the pre-ZLB period, and 8.9% for the ZLB period. Most of these improvements in RMSE are observed for the three-month, one-year, two-year, five-year and ten-year yields, whereas for the other maturities there is a slight deterioration in fit.

Lastly, the AFNS model performs slightly worse than the original DNS model for five out of eight maturities during the total and pre-ZLB period, and for four out of eight

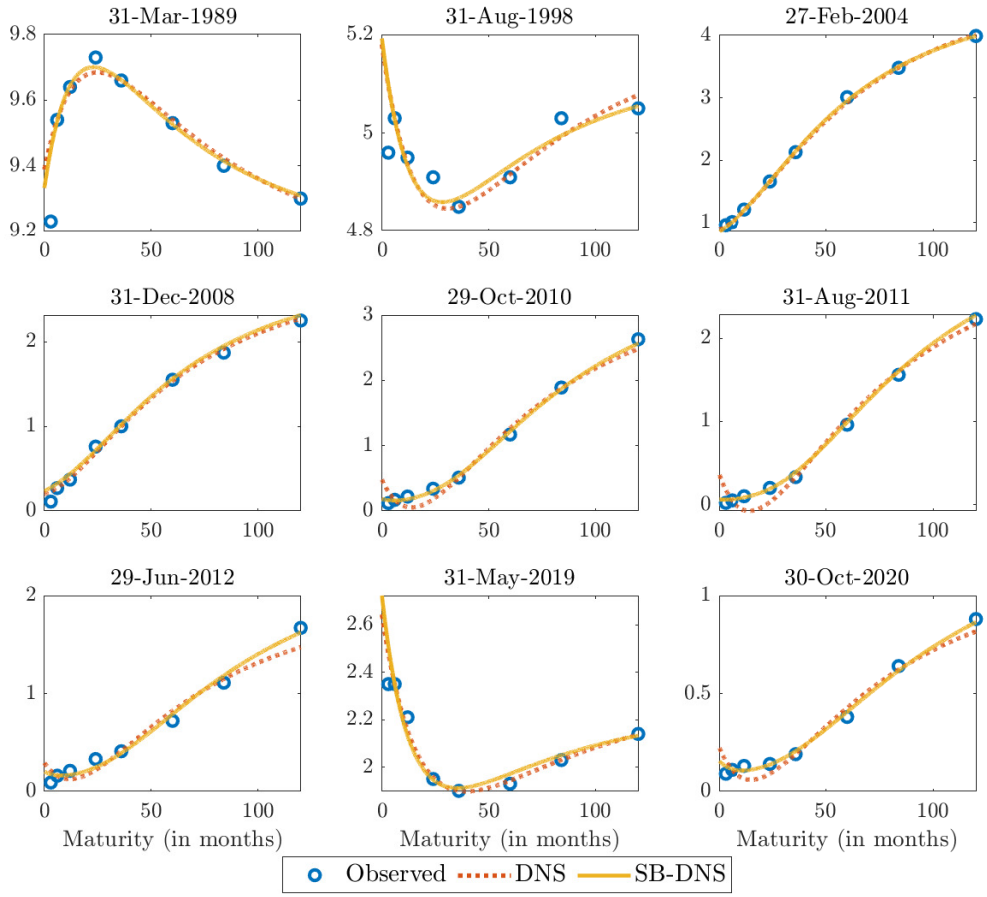

Figure 5: Yield curve fit and observations across maturities (in months) for nine selected dates

maturities during the ZLB period. Nonetheless, the total RMSE, taking all maturities into account, is smaller for AFNS than for the DNS model in all three periods. The B-AFNS model performs substantially better than the AFNS model, particularly during the ZLB period with a decrease in total RMSE of 28.8%. The RMSEs of the B-AFNS model are close to the ones of the SB-DNS model for most maturities. Looking at the total RMSEs, they are the same for the total period and the pre-ZLB period, but lower for the SB-DNS model during the ZLB period. To examine this further, Figure 6 plots the residuals of four models: DNS, SB-DNS, AFNS and B-AFNS. The residuals of the SB-DNS and B-AFNS are close to each other and both improve upon the DNS and AFNS models during certain parts of the ZLB period, particularly for the three-month, one-year and ten-year maturities. Hence, the SB-DNS model is competitive with the more rigorous class of shadow-rate affine term structure models in terms of in-sample fit.

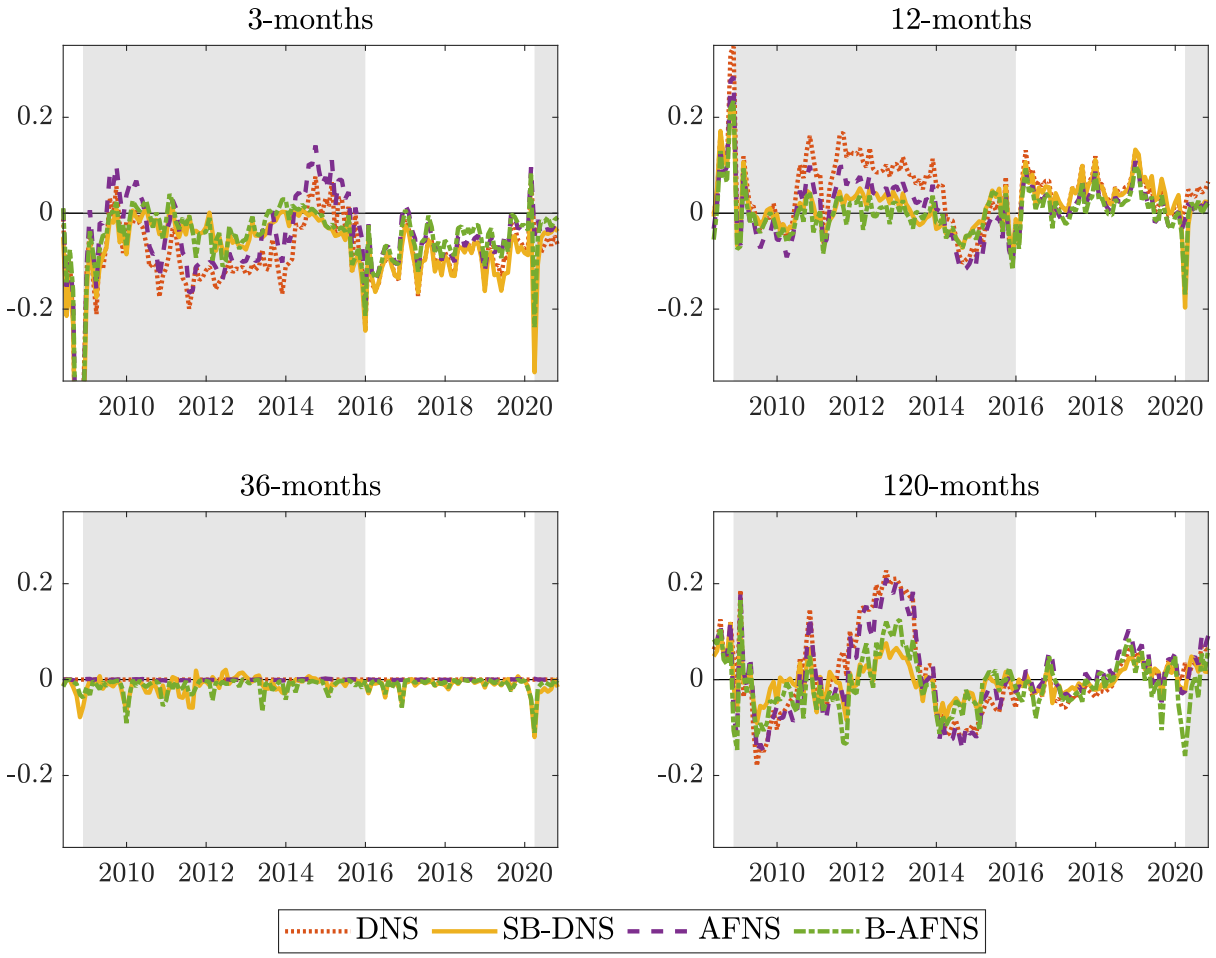

Figure 6: Time series of yield curve residuals across maturities in the post-GFC period with shaded ZLB periods

4.2 Why do we need to impose the ZLB?

Beside the inferior in-sample fit of the plain DNS model compared to the shadow-rate models, we show in this subsection that the DNS model also lacks the ability to generate plausible future yield curve behaviour at the ZLB, which is also found for the plain affine term structure models. First, Figure 7 displays the conditional probabilities of negative three-month ahead yields from the DNS model, based on 10,000 simulations at each observation date t. Prior to the GFC, all yields have negligible probabilities of turning into negative territory, except perhaps for the three-month yield around 2004. However, the probabilities of the three-month and two-year yields increase substantially during the ZLB period. In fact, even the ten-year yield shows positive probabilities close to 0.2 after the corona virus pandemic hit the U.S. Hence, by ignoring the ZLB, the DNS model is not able to generate realistic future interest rate paths as U.S. interest rates did not become negative during our sample with a minimum of 0.55 for the ten-year yields (see Table 1).

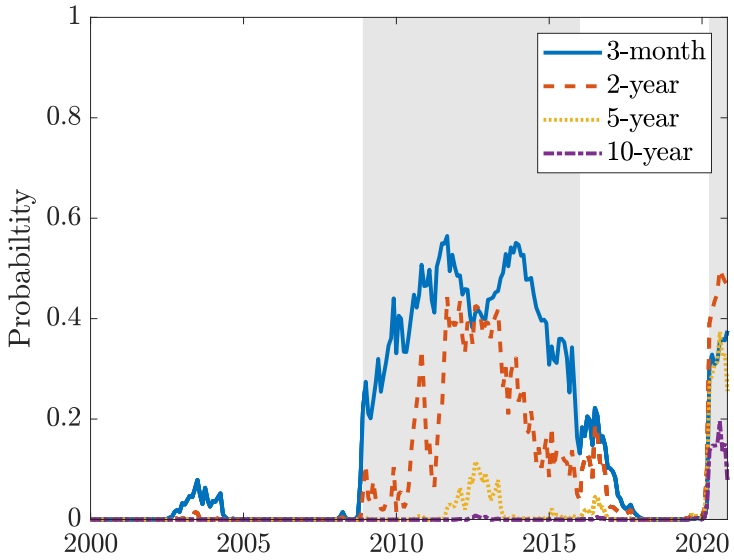

Figure 7: Conditional probabilities of negative three-month ahead yields from the DNS model with shaded ZLB periods

These unlikely high positive probabilities of negative interest rates are also found for the standard affine term structure model class, see Christensen and Rudebusch (2015, 2016) and Bauer and Rudebusch (2016), among others.

Second, we address the inability of the DNS model to capture yield-curve compression at the ZLB. Figure 8 shows the conditional volatility of three-month ahead yields obtained from the DNS, B-DNS and SB-DNS models, based on 10,000 simulations at each observation date t. For comparison, we also include a realized-volatility (RV) measure, where we follow Christensen and Rudebusch (2016) and compute rolling standard deviations of daily yield changes over the number of trading days in the next 91-day window. Due to the linearity of the DNS measurement equation and the convergence of the covariance matrix of the latent factors, we expect that the DNS model produces constant yield volatility, which is indeed found in Figure 8 with a level close to 0.6. However, for both the three-month and two-year yield, the RV measure decreases drastically after the GFC to a level of 0.1-0.2. Meanwhile, the SB-DNS model is able to replicate this decrease in volatility and sticks more closely to the RV measure, although there is some divergence of the series between the two ZLB periods. The B-DNS model is partly able to capture the volatility compression, but it converges rather quickly to the constant volatility level of the DNS model. Overall, the DNS model is not able to capture the observed yield volatility compression at the ZLB, while the SB-DNS model can accurately replicate this compression. These shortcomings in capturing the low yield volatility is also found for the

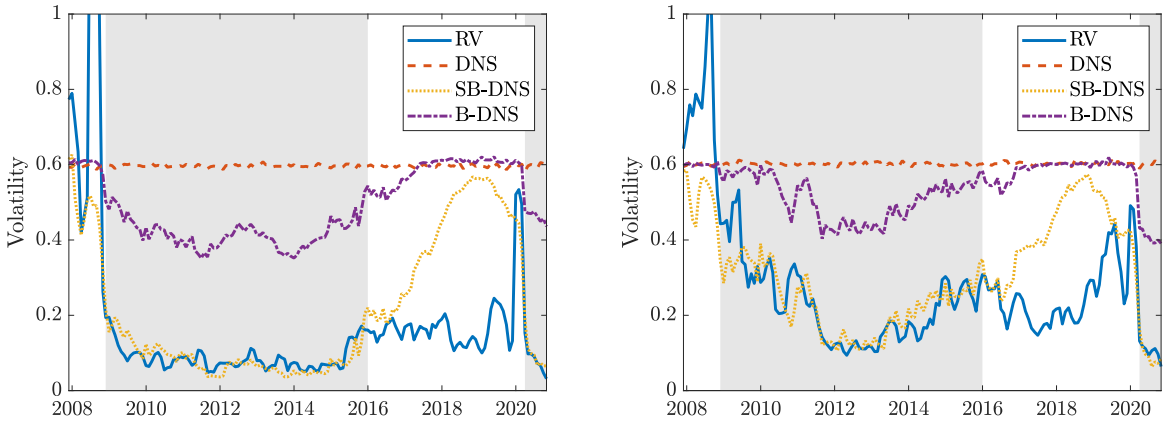

(a) Three-month yield **(b)** Two-year yield

Figure 8: Three-month ahead realized and model-implied conditional volatility series of yields in the post-GFC period with shaded ZLB periods

standard affine term structure model (Christensen and Rudebusch, 2015, 2016), which is then resolved with the shadow-rate affine term structure model.

4.3 Policy insights at the ZLB

In this subsection we provide some policy insights at the ZLB that can be obtained from our smooth shadow-rate DNS model. More specifically, we first examine and compare the estimated shadow short rates, which some advocate to be a useful measure of the stance of unconventional monetary policy at the ZLB (Bullard, 2012; Krippner, 2013; Wu and Xia, 2016; Francis et al., 2020). Indeed, quite some recent work has adopted shadow short-rate estimates to assess the efficiency of (un)conventional monetary policy (Damjanović and Masten, 2016; von Borstel et al., 2016; Ouerk et al., 2020). Nonetheless, Christensen and Rudebusch (2015, 2016) and Krippner (2020) show that shadow short-rate estimates are highly sensitive to choices in their estimation such as the model specification and the used data. Unsurprisingly, in Appendix E we show that the level of our shadow short rate estimates are also highly sensitive to the lower bound and smoothness parameter specifications. Hence, these estimates should always be employed with caution.

Figure 9 shows the filtered shadow short rates based on the SB-DNS model with a fixed lower-bound specification of 0% and a smoothness parameter γ that is either estimated or fixed at a value of 1. For comparison, we also include the filtered shadow short rate of the B-AFNS model and the estimates from Wu and Xia (2016).[18] Four

[18]The shadow short-rate estimate of Wu and Xia (2016) can be obtained from the website of Jing

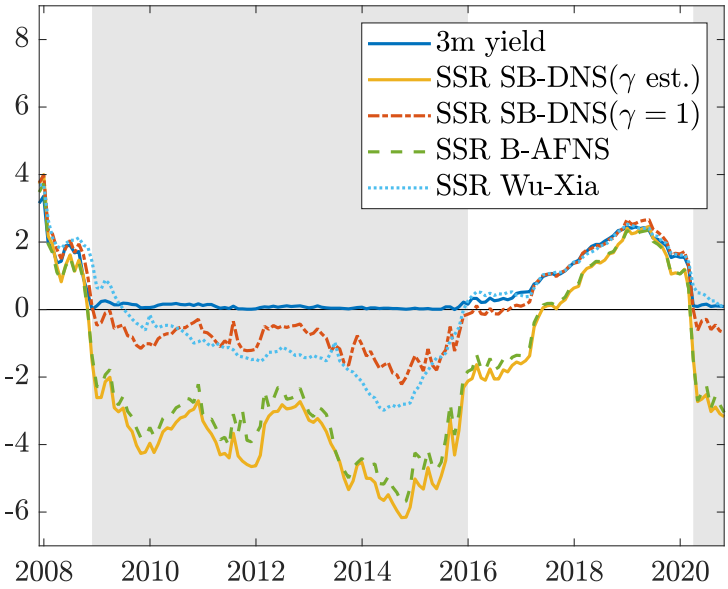

Figure 9: Shadow short rate estimates in the post-GFC period with shaded ZLB periods

things stand out. First, all shadow short-rate estimates are close to the three-month yield when it is not close to the ZLB, where they start to diverge closer to the ZLB. Second, the SB-DNS model with an estimated smoothness parameter generates a filtered shadow short rate that is highly similar to the one of the B-AFNS model in terms of dynamics and level. In fact, their correlation is 0.998, while the correlation of their first differences is 0.942. Third, the filtered shadow short rate of the SB-DNS model with a fixed smoothness parameter of $\gamma = 1$ resembles the estimate from Wu and Xia (2016) in terms of level, even though the latter is obtained from a shadow-rate affine term structure model estimated with forward-rate data and a lower-bound specification of 0.25%. The correlation of their levels and first differences are 0.935 and 0.600, respectively. Lastly, in Appendix E we additionally show that our shadow short-rate estimate based on a two-factor smooth shadow-rate model, which Krippner (2015a) argues to produce more robust and economically meaningful estimates, are close to the ones based on Krippner (2015a).[19] Overall, the SB-DNS model is thus able to generate similar shadow short-rate estimates, in terms of dynamics and level, as are currently produced in the literature.

Another policy-related measure that can be obtained from the SB-DNS model is the liftoff horizon that indicates the timing of future policy liftoff, see Bauer and Rudebusch (2016) for further details. Figure 10 shows the median and interquartile range (IQR)

Cynthia Wu: https://sites.google.com/view/jingcynthiawu/shadow-rates.

[19]The shadow short rate estimates of Krippner (2015a) can be obtained from the website of Leo Krippner: https://www.ljkmfa.com/visitors/.

liftoff-horizon estimates (in years) obtained from the SB-DNS model with an estimated smoothness parameter γ, based on 10,000 simulations at each observation date t. Similarly as Lemke and Vladu (2017), we identify a liftoff date as the initial time that the projected short rate is above the threshold of 25 basis points, which corresponds to the 0 to 25 basis points range of the Federal Reserve during the ZLB period, and stays there for 12 consecutive months.[20] Figure 10 indicates that the liftoff horizon is increasing after the GFC, but that it starts to decrease almost linearly from 2013 onwards until the end of the ZLB period. The median liftoff horizon is close to the realized liftoff line and generally within the IQR, albeit the predicted liftoff date has a delay of about six months. Noteworthy, the liftoff horizon increased dramatically at the start of the corona virus pandemic, although it starts to decrease again from mid-2020 onwards. Hence, this suggests that it will take quite some years before the policy rate is lifted from the ZLB again.

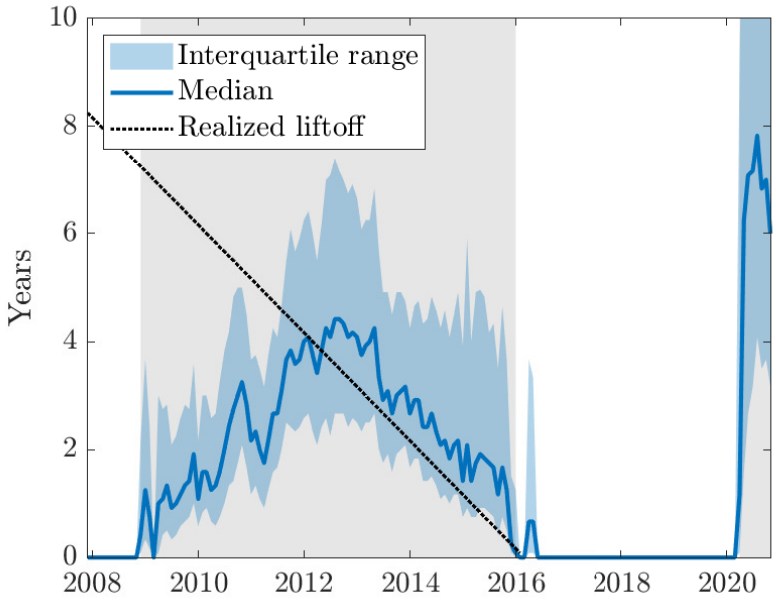

Figure 10: Liftoff horizon estimates from the SB-DNS model (including the realized liftoff horizon) in the post-GFC period with shaded ZLB periods

[20] Note that the model-implied short rate under the SB-DNS model is given by $r_t = r_{LB} + \gamma f\left(\frac{s_t - r_{LB}}{\gamma}\right)$.

4.4 Forecasting the yield curve

Finally, we assess the out-of-sample performance of the smooth shadow-rate model and compare it to the other models. Similarly as Christensen and Rudebusch (2016), we employ expanding-window estimation with an initial estimation sample from September 1981 to August 2001 (240 observations).[21] By adding one month of observations each time, we conduct a total of 231 estimations per model. Across all estimations, we assume a fixed lower-bound specification of 0% and a fixed smoothness parameter of 1.[22] This prefixing of lower bound and smoothness parameters is necessary to circumvent overfitting issues that would happen when the shadow-rate models are estimated over a period with only high interest-rate data. Then, at each end date of the estimation sample, we construct one-month-ahead ($h = 1$), six-month-ahead ($h = 6$), one-year-ahead ($h = 12$) and two-year-ahead ($h = 24$) forecasts. As a result, we obtain 230 one-month-ahead forecasts, 225 six-month-ahead forecasts, 219 one-year-ahead forecasts and 207 two-year-ahead forecasts that can be evaluated. For each forecast horizon and maturity, we compute the root mean squared forecast errors (RMSFE).

Table 4 displays the RMSFE of all models across the four horizons and eight maturities. Beside the six model forecasts, we also include random walk forecasts, which are known to be a hard-to-beat benchmark for yields (Duffee, 2002). Indeed, we find that the DNS model is outperformed by the random walk forecasts for almost all forecast horizons and yield maturities. In fact, the random walk forecasts seem to outperform most models, particularly for shorter horizon forecasts. This outperformance of the random walk also becomes clear from the cumulative sum of squared forecast errors (CSSFE) plots for six-months-ahead and two-year-ahead forecasts in Figures 11 and 12, respectively.[23]

Most prominently, we find that the SB-DNS model outperforms the DNS model for all horizons and maturities, where this improvement is strongest for longer horizons. Moreover, the SB-DNS model is also able to outperform the random walk for longer horizon forecasts of short-term yields. Figure 12 shows that his outperformance of the SB-DNS model for the two-year ahead forecasts mostly stems from the beginning of the

[21] Alternatively, Appendix G.1 includes the rolling-window estimation results, where the (SB-)DNS-type models slightly deteriorate in accuracy relative to the(B-)AFNS-type models. Still, the best performing forecasts for most models are generally based on the expanding-window estimation approach.

[22] For relaxations of these lower-bound and smoothness parameter specifications in the forecasting exercise, see Appendices D and F, respectively.

[23] The CSSFEs for one-month-ahead and one-year-ahead forecasts are given in Appendix G.2.

Table 4: Out-of-sample performance

RMSFE	**Maturities (in months)**							
	3	**6**	**12**	**24**	**36**	**60**	**84**	**120**
Panel A: One-month-ahead forecasts (h = 1)								
RW	**20.5**	19.3	19.4	**22.7**	**24.7**	26.3	**26.4**	**25.5**
DNS	24.9	18.7	19.9	23.7	25.6	27.3	27.2	26.9
DNS-TVL	25.0	19.3	**18.6**	23.2	26.2	27.2	27.4	26.6
B-DNS	25.4	19.1	19.8	23.7	25.7	27.4	27.2	26.9
SB-DNS	22.6	**18.4**	19.5	23.6	25.6	26.9	27.1	26.0
SB-DNS-TVL	24.1	19.1	18.8	23.3	25.9	26.9	27.2	26.1
AFNS	34.5	29.9	29.3	29.7	29.0	26.6	28.1	27.0
B-AFNS	21.1	21.7	22.4	24.2	25.3	**26.0**	26.8	26.1
Panel B: Six-month-ahead forecasts (h = 6)								
RW	66.8	66.7	**65.3**	**66.1**	**67.3**	65.8	63.5	60.0
DNS	69.6	68.1	68.6	73.1	75.9	75.1	71.7	68.3
DNS-TVL	74.5	71.5	71.7	76.1	79.7	78.7	75.2	71.5
B-DNS	70.8	68.9	68.7	72.4	74.8	74.0	70.7	67.4
SB-DNS	**62.7**	**65.3**	67.2	70.8	72.6	71.1	67.7	63.0
SB-DNS-TVL	70.7	69.5	70.3	74.3	76.7	74.5	70.7	66.1
AFNS	123.4	118.0	113.7	106.5	97.5	79.4	72.6	62.9
B-AFNS	72.8	74.9	73.8	72.3	70.2	**64.6**	**62.0**	**57.6**
Panel C: One-year-ahead forecasts (h = 12)								
RW	116.5	115.1	109.6	**101.4**	**95.9**	86.8	81.4	75.5
DNS	118.2	116.7	116.0	116.5	115.9	109.6	103.3	97.6
DNS-TVL	121.7	119.3	119.3	120.6	121.0	114.6	107.7	101.6
B-DNS	117.0	115.1	113.2	112.2	111.1	105.0	99.2	94.1
SB-DNS	**107.1**	**109.4**	**109.2**	107.8	105.8	98.7	92.4	84.8
SB-DNS-TVL	116.9	116.0	115.8	115.6	113.9	105.0	97.6	90.7
AFNS	187.8	182.2	177.9	166.3	150.3	117.9	102.5	85.0
B-AFNS	110.6	112.0	109.9	104.7	98.0	**84.6**	**79.9**	**73.7**
Panel D: Two-year-ahead forecasts (h = 24)								
RW	191.4	190.9	181.1	161.6	146.8	124.4	**110.4**	97.5
DNS	201.2	199.1	194.6	186.6	180.0	165.5	152.9	141.5
DNS-TVL	193.2	190.7	189.1	185.5	181.9	169.2	156.8	146.1
B-DNS	189.0	186.5	180.7	171.0	163.8	149.8	138.2	128.7
SB-DNS	**170.1**	**170.3**	**165.2**	**155.8**	149.9	137.7	125.8	111.5
SB-DNS-TVL	185.1	183.4	181.1	175.5	170.0	155.0	141.7	129.8
AFNS	264.3	257.7	251.3	232.2	207.6	159.7	132.6	104.5
B-AFNS	176.6	175.7	170.3	158.2	**145.8**	**123.5**	111.2	**97.3**

Notes: This table contains the Root Mean Squared Forecasts Errors (RMSFE) in basis points across maturities and forecast horizons. We consider expanding-window estimation with the initial sample from September 1981 to Augustus 2001 (240 observations) resulting in 230 one-month-ahead forecasts, 225 six-month-ahead forecasts, 219 one-year-ahead forecasts and 207 two-year-ahead forecasts to compute the RMSFEs. The shadow-rate models are all estimated with a fixed lower bound specification of $r_{LB} = 0\%$, while the smooth shadow-rate model has a fixed smoothness parameter $\gamma = 1$. The bold numbers indicate the lowest RMSFE for that particular maturity and horizon.

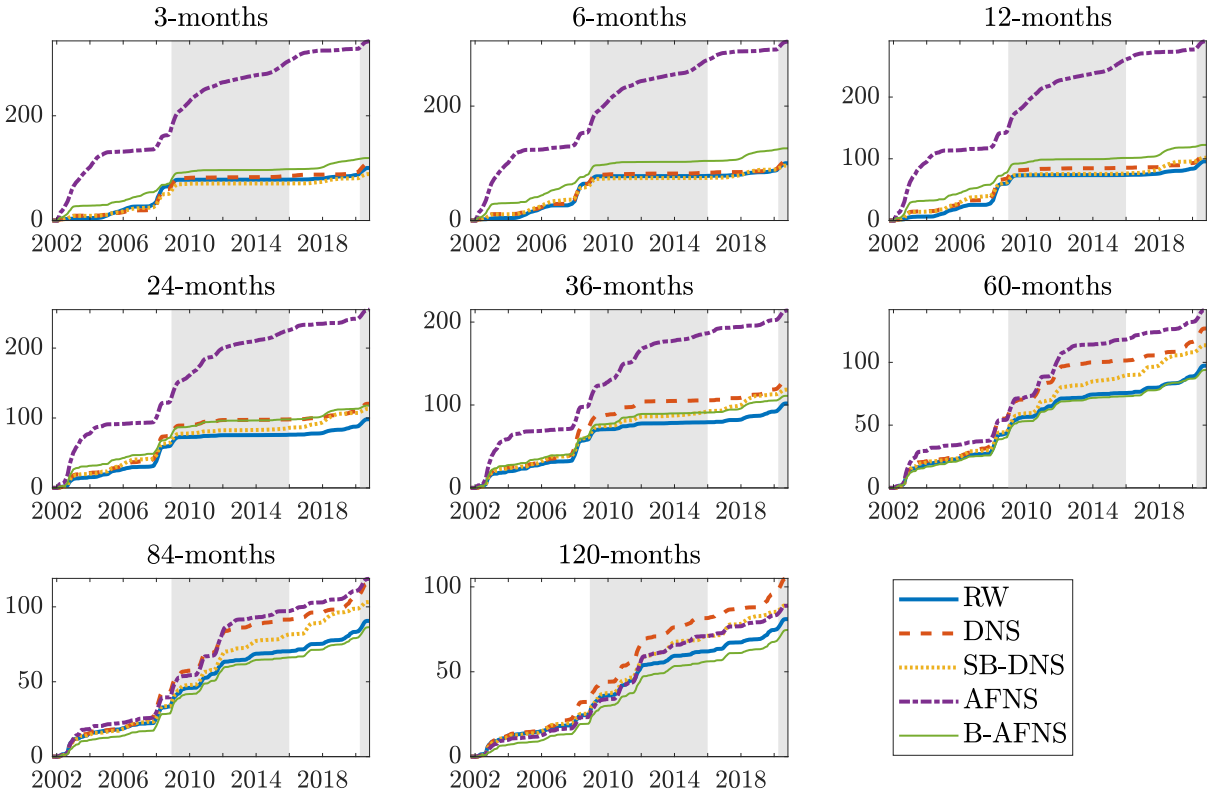

Figure 11: Cumulative sum of squared forecast errors for six-month ahead forecasts with shaded ZLB periods

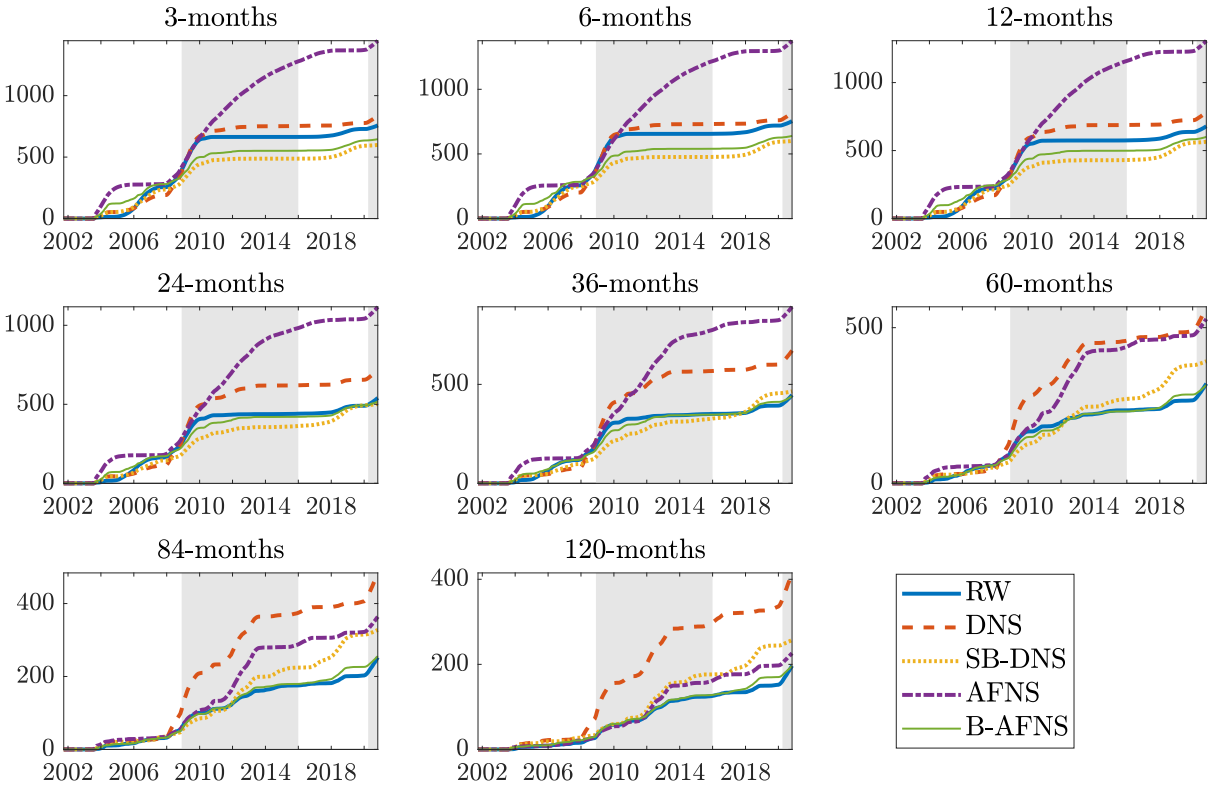

Figure 12: Cumulative sum of squared forecast errors for two-year ahead forecasts with shaded ZLB periods

ZLB period. Hence, imposing the smooth shadow-rate restriction, and thereby allowing for a smooth transition into the ZLB state, substantially improves the out-of-sample performance, especially compared to the baseline DNS and B-DNS models.

Moving to the time-varying loading models, we find that these generally do not outperform their constant loading counterparts. More specifically, the DNS model often performs better than the DNS-TVL model, while the SB-DNS model performs better than the SB-DNS-TVL model. So, despite that allowing for time-varying loadings seems to improve the in-sample fit, this comes at the cost of poorer forecasting performance. This result could be due to additional forecasting uncertainty as the TVL models also need to predict the time-varying loadings, but it might also indicate that the TVL models are prone to overfitting. By looking at subperiods in Appendix G.3, though, we find that during non-ZLB periods the (SB-)DNS-TVL model performs somewhat better for several maturities and horizons.

Next, the out-of-sample performance of the SB-DNS model is compared to the AFNS and B-AFNS models. We find that the SB-DNS model performs better than the AFNS and B-AFNS models for longer horizons and short-term yields. Yet, the B-AFNS model performs substantially better for long-term yields, which could be due to the yield adjustment term of the (B-)AFNS expression (Christensen et al., 2011). The B-AFNS model, in turn, outperforms the AFNS model across all horizons and maturities, which is consistent with the results of Christensen and Rudebusch (2016). Also, the AFNS is able to outperform the DNS model for long-term yields and long forecast horizons, although the AFNS performance quickly deteriorates for short-term yields, which becomes also clear from Figures 11 and 12. To summarize, we conclude that the SB-DNS model is competitive with the B-AFNS model for short- and medium term yield forecasts, but is lacking for longer maturities.

Lastly, we test the significance of the forecasting accuracy of the SB-DNS model against its competitors by means of Diebold and Mariano (1995) (DM) tests. The null hypothesis is that the two competing forecasts are equally accurate, while the alternative hypothesis states that the forecast with a lower RMSFE is significantly more accurate. The test statistic is obtained as the average difference between the RMSFE of the SB-DNS and its competitor, divided by the square of the long-run variance of these differentials, based on the Bartlett kernel with automatic bandwidth selection as in Newey and West

Table 5: Significance of SB-DNS forecasting performance over alternatives

DM stat.	**Maturities (in months)**							
	3	**6**	**12**	**24**	**36**	**60**	**84**	**120**
Panel A: One-month-ahead forecasts (h = 1)								
RW	0.92	-0.89	0.11	1.25	**2.76*****	1.57*	**1.72****	**1.74****
DNS	**-4.11*****	-0.59	-0.51	-0.27	0.05	-1.14	-0.10	**-2.21****
DNS-TVL	**-4.72*****	-1.26	1.02	0.41	-0.99	-0.81	-0.73	-0.87
B-DNS	**-3.95*****	-1.15	-0.44	-0.24	-0.09	-1.18	-0.24	**-2.19****
SB-DNS-TVL	**-2.90*****	-1.03	0.83	0.32	-0.58	0.27	-0.14	-0.04
AFNS	**-4.98*****	**-4.02*****	**-3.21*****	**-3.01*****	**-3.15*****	1.20	**-1.89****	**-2.44*****
B-AFNS	0.74	**-2.02****	**-2.14****	-0.65	0.73	1.37*	1.05	-0.21
Panel B: Six-month-ahead forecasts (h = 6)								
RW	-0.91	-0.27	0.39	1.28	**1.72****	**2.04****	**1.73****	1.30*
DNS	-1.43*	-0.58	-0.28	-0.53	-0.81	-1.14	-1.16	**-1.65****
DNS-TVL	**-1.87****	-0.94	-0.68	-0.93	-1.49*	**-1.84****	**-1.79****	**-1.98****
B-DNS	-1.52*	-0.71	-0.30	-0.33	-0.52	-0.79	-0.81	-1.26
SB-DNS-TVL	-1.38*	-0.71	-0.52	-0.67	-0.94	-0.91	-0.79	-0.79
AFNS	**-4.71*****	**-4.04*****	**-3.76*****	**-3.57*****	**-3.39*****	**-2.06****	-1.38*	0.05
B-AFNS	**-1.71****	**-1.82****	-1.43*	-0.47	1.18	**3.21*****	**2.62*****	**2.28****
Panel C: One-year-ahead forecasts (h = 12)								
RW	-1.02	-0.56	-0.05	0.83	1.50*	**2.19****	**2.18****	**1.96****
DNS	-1.09	-0.73	-0.68	-0.91	-1.09	-1.31*	-1.39*	**-1.74****
DNS-TVL	-1.31*	-0.84	-0.89	-1.28	**-1.71****	**-1.98****	**-1.92****	**-2.08****
B-DNS	-1.02	-0.60	-0.43	-0.50	-0.62	-0.78	-0.87	-1.21
SB-DNS-TVL	-0.97	-0.63	-0.65	-0.86	-0.97	-0.79	-0.63	-0.68
AFNS	**-4.27*****	**-3.73*****	**-3.64*****	**-3.63*****	**-3.46*****	**-2.30****	-1.50*	-0.05
B-AFNS	-0.44	-0.35	-0.10	0.61	**2.17****	**4.03*****	**3.19*****	**2.75*****
Panel D: Two-year-ahead forecasts (h = 24)								
RW	-1.51*	-1.40*	-1.15	-0.47	0.26	1.27	1.60*	1.62*
DNS	-1.64*	-1.55*	-1.57*	**-1.67****	**-1.70****	**-1.72****	**-1.78****	**-2.09****
DNS-TVL	-1.43*	-1.23	-1.48*	**-1.99****	**-2.31****	**-2.54*****	**-2.66*****	**-3.12*****
B-DNS	-1.25	-1.07	-1.01	-1.00	-0.94	-0.86	-0.90	-1.27
SB-DNS-TVL	-1.10	-0.95	-1.16	-1.51*	-1.57*	-1.36*	-1.25	-1.45*
AFNS	**-4.08*****	**-3.68*****	**-3.76*****	**-3.82*****	**-3.42*****	**-1.84****	-0.70	1.13
B-AFNS	-0.85	-0.74	-0.72	-0.36	0.63	**2.21****	**2.32****	**2.45*****

Notes: This table contains the Diebold and Mariano (1995) (DM) test statistics of the SB-DNS model against its competitors. The null hypothesis of the test is that the two competing forecasts are equally accurate, while the alternative hypothesis states that the forecast with a lower RMSFE is significantly more accurate. A negative value indicates that the RMSFE of the SB-DNS model is lower than the one of its competitor. The test statistic is obtained as the average difference between the RMSFE of the SB-DNS and its competitor, divided by the square of the long-run variance of these differentials, based on the Bartlett kernel with automatic bandwidth selection as in Newey and West (1994). The asterisks $*$,$**$, and $***$ indicate significance at the 10%, 5% and 1% level, respectively. A bold number indicates significance at the 5% level.

(1994). Table 5 presents the DM statistics and the corresponding significance at the 1%, 5% and 10% levels. We find a large number of negative values, which indicate that the SB-DNS model outperforms its competitors. The outperformance over the DNS and DNS-TVL models is mostly significant for longer horizons and maturities, but also for the three-month yield at shorter horizons. In addition, the AFNS model is significantly outperformed at almost all maturities and horizons, while the B-AFNS is outperformed at the short-end of the yield curve for short horizons. Still, the B-AFNS significantly outperforms the SB-DNS model for longer horizons and maturities, whereas the random walk generally outperforms for short horizons. Hence, it ultimately depends on the horizon and maturity which model performs best.

5 Conclusion

In this paper we develop a smooth shadow-rate version of the dynamic Nelson-Siegel (DNS) model to analyze and forecast U.S. government bond yields during the recent zero lower bound (ZLB) periods. Our smooth shadow-rate DNS model has a closed-form yield curve expression and hence can be easily put into a nonlinear state-space form to facilitate tractable estimation. Consequently, it is straightforward to extend our model with time-varying parameters, macroeconomic variable integration or other variations of interest, which are not always possible in the more rigorous and less tractable class of shadow-rate affine term structure models.

Our results show that the smooth shadow-rate DNS (SB-DNS) model dominates the original DNS model in terms of fitting and forecasting the yield curve with better out-of-sample performance for all yield maturities and forecast horizons. The SB-DNS model is also competitive with the shadow-rate affine term structure models in fitting and forecasting the yield curve for short- and medium-term maturities, particularly for longer horizons. Furthermore, we provide evidence of a smooth transition of the term structure of interest rates entering and leaving the ZLB state, indicated by a highly significant smoothness parameter and improved in- and out-of-sample performance of the smooth shadow-rate model over a non-smooth version. Finally, we show that the DNS model lacks in generating plausible future yield curve paths, which can be resolved with the smooth shadow-rate augmentation, and we illustrate how the smooth shadow-rate model can be used to shape future policy expectations at the ZLB.

References

Abdymomunov, A., K. H. Kang, and K. J. Kim (2016): "Can credit spreads help predict a yield curve?" *Journal of International Money and Finance*, 64, 39–61.

Andreasen, M. M. and A. Meldrum (2019): "A Shadow Rate or a Quadratic Policy Rule? The Best Way to Enforce the Zero Lower Bound in the United States," *Journal of Financial and Quantitative Analysis*, 54, 2261–2292.

Ansley, C. F. and R. Kohn (1986): "A note on reparameterizing a vector autoregressive moving average model to enforce stationarity," *Journal of Statistical Computation and Simulation*, 24, 99–106.

Bauer, M. D. and G. D. Rudebusch (2016): "Monetary Policy Expectations at the Zero Lower Bound," *Journal of Money, Credit and Banking*, 48, 1439–1465.

Black, F. (1995): "Interest Rates as Options," *The Journal of Finance*, 50, 1371–1376.

Bomfim, A. N. (2003): "Interest rates as options: assessing the markets' view of the liquidity trap," Tech. Rep. 2003-45, Board of Governors of the Federal Reserve System (US).

Bullard, J. B. (2012): "Shadow interest rates and the stance of U.S. monetary policy," Tech. Rep. 206, Federal Reserve Bank of St. Louis, publication Title: Speech.

Byrne, J. P., S. Cao, and D. Korobilis (2017): "Forecasting the term structure of government bond yields in unstable environments," *Journal of Empirical Finance*, 44, 209–225.

Caldeira, J. F., M. P. Laurini, and M. S. Portugal (2010): "Bayesian Inference Applied to Dynamic Nelson-Siegel Model with Stochastic Volatility," *Brazilian Review of Econometrics*, 30, 123–161.

Christensen, J. H., F. X. Diebold, and G. D. Rudebusch (2011): "The affine arbitrage-free class of Nelson–Siegel term structure models," *Journal of Econometrics*, 164, 4–20.

Christensen, J. H. E. (2015): "A Regime-Switching Model of the Yield Curve at the Zero Bound," *Federal Reserve Bank of San Francisco, Working Paper Series*, 01–63.

Christensen, J. H. E. and G. D. Rudebusch (2015): "Estimating Shadow-Rate Term Structure Models with Near-Zero Yields," *Journal of Financial Econometrics*, 13, 226–259.

——— (2016): "Modeling Yields at the Zero Lower Bound: Are Shadow Rates the Solution?" *Dynamic Factor Models*, 35, 75–125.

Chung, T.-K., C.-H. Hui, and K.-F. Li (2017): "Term-structure modelling at the zero lower bound: Implications for estimating the forward term premium," *Finance Research Letters*, 21, 100–106.

Chung, T.-K. and H. Iiboshi (2015): "Prediction of Term Structure with Potentially Misspecified Macro-Finance Models near the Zero Lower Bound," Tech. Rep. 85709, University Library of Munich, Germany.

Coroneo, L., D. Giannone, and M. Modugno (2016): "Unspanned Macroeconomic Factors in the Yield Curve," *Journal of Business & Economic Statistics*, 34, 472–485.

Coroneo, L., K. Nyholm, and R. Vidova-Koleva (2011): "How arbitrage-free is the Nelson–Siegel model?" *Journal of Empirical Finance*, 18, 393–407.

Cox, J. C., J. E. Ingersoll, and S. A. Ross (1985): "A Theory of the Term Structure of Interest Rates," *Econometrica*, 53, 385.

Dai, Q. and K. J. Singleton (2000): "Specification Analysis of Affine Term Structure Models," *The Journal of Finance*, 55, 1943–1978.

Damjanović, M. and I. Masten (2016): "Shadow short rate and monetary policy in the Euro area," *Empirica*, 43, 279–298.

Diebold, F. X. and C. Li (2006): "Forecasting the term structure of government bond yields," *Journal of Econometrics*, 130, 337–364.

Diebold, F. X. and R. S. Mariano (1995): "Comparing Predictive Accuracy," *Journal of Business & Economic Statistics*, 13, 253–263.

Diebold, F. X. and G. D. Rudebusch (2013): *Yield Curve Modeling and Forecasting: The Dynamic Nelson-Siegel Approach*, Princeton University Press.

Diebold, F. X., G. D. Rudebusch, and S. Boragan Aruoba (2006): "The macroeconomy and the yield curve: a dynamic latent factor approach," *Journal of Econometrics*, 131, 309–338.

Dijk, D. v., S. J. Koopman, M. v. d. Wel, and J. H. Wright (2014): "Forecasting interest rates with shifting endpoints," *Journal of Applied Econometrics*, 29, 693–712.

Duffee, G. (2011): "Forecasting with the term structure: The role of no-arbitrage restrictions," Tech. Rep. 576, The Johns Hopkins University,Department of Economics, publication Title: Economics Working Paper Archive.

Duffee, G. R. (2002): "Term Premia and Interest Rate Forecasts in Affine Models," *The Journal of Finance*, 57, 405–443.

Duffie, D. and R. Kan (1996): "A Yield-Factor Model of Interest Rates," *Mathematical Finance*, 6, 379–406.

Durbin, J. and S. J. Koopman (2012): *Time Series Analysis by State Space Methods*, Oxford University Press, 2 ed.

Exterkate, P., D. V. Dijk, C. Heij, and P. J. F. Groenen (2013): "Forecasting the Yield Curve in a Data-Rich Environment Using the Factor-Augmented Nelson–Siegel Model," *Journal of Forecasting*, 32, 193–214.

Filipović, D., M. Larsson, and A. B. Trolle (2017): "Linear-Rational Term Structure Models: Linear-Rational Term Structure Models," *The Journal of Finance*, 72, 655–704.

Francis, N. R., L. E. Jackson, and M. T. Owyang (2020): "How has empirical monetary policy analysis in the U.S. changed after the financial crisis?" *Economic Modelling*, 84, 309–321.

Gorovoi, V. and V. Linetsky (2004): "Black's model of interest rates as options, eigenfunction expansions and japanese interest rates," *Mathematical Finance*, 14, 49–78.

Hamilton, J. D. (1994): "State-space models," in *Handbook of Econometrics*, Elsevier, vol. 4, 3039–3080.

Han, Y., A. Jiao, and J. Ma (2021): "The predictive power of Nelson-Siegel factor loadings for the real economy," *Journal of Empirical Finance*, Forthcoming.

Hautsch, N. and Y. Ou (2012): "Analyzing interest rate risk: Stochastic volatility in the term structure of government bond yields," *Journal of Banking & Finance*, 36, 2988–3007.

Hautsch, N. and F. Yang (2012): "Bayesian inference in a Stochastic Volatility Nelson–Siegel model," *Computational Statistics & Data Analysis*, 56, 3774–3792.

Hevia, C., M. Gonzalez-Rozada, M. Sola, and F. Spagnolo (2015): "Estimating and Forecasting the Yield Curve Using A Markov Switching Dynamic Nelson and Siegel Model," *Journal of Applied Econometrics*, 30, 987–1009.

Ichiue, H. and Y. Ueno (2007): "Equilibrium Interest Rate and the Yield Curve in a Low Interest Rate Environment," Bank of Japan Working Paper Series 07-E-18, Bank of Japan.

Kang, K. H. (2015): "The predictive density simulation of the yield curve with a zero lower bound," *Journal of Empirical Finance*, 33, 51–66.

Kim, D. H. and K. J. Singleton (2012): "Term structure models and the zero bound: An empirical investigation of Japanese yields," *Journal of Econometrics*, 170, 32–49.

Koopman, S. J., M. I. P. Mallee, and M. Van der Wel (2010): "Analyzing the Term Structure of Interest Rates Using the Dynamic Nelson–Siegel Model With Time-Varying Parameters," *Journal of Business & Economic Statistics*, 28, 329–343.

Koopman, S. J. and M. van der Wel (2013): "Forecasting the US term structure of interest rates using a macroeconomic smooth dynamic factor model," *International Journal of Forecasting*, 29, 676–694.

Kortela, T. (2016): "A shadow rate model with time-varying lower bound of interest rates," Tech. Rep. 19/2016, Bank of Finland.

Krippner, L. (2012): "Modifying Gaussian term structure models when interest rates are near the zero lower bound," *CAMA Working Papers*, 48.

——— (2013): "Measuring the stance of monetary policy in zero lower bound environments," *Economics Letters*, 118, 135–138.

——— (2015a): "A comment on Wu and Xia (2015), and the case for two-factor Shadow Short Rates," Tech. Rep. 2015-48, Centre for Applied Macroeconomic Analysis, Crawford School of Public Policy, The Australian National University, publication Title: CAMA Working Papers.

——— (2015b): "A Theoretical Foundation for the Nelson–Siegel Class of Yield Curve Models," *Journal of Applied Econometrics*, 30, 97–118.

——— (2020): "A Note of Caution on Shadow Rate Estimates," *Journal of Money, Credit and Banking*, 52, 951–962.

Laurini, M. P. and J. F. Caldeira (2016): "A macro-finance term structure model with multivariate stochastic volatility," *International Review of Economics & Finance*, 44, 68–90.

Laurini, M. P. and L. K. Hotta (2010): "Bayesian extensions to Diebold-Li term structure model," *International Review of Financial Analysis*, 19, 342–350.

Lemke, W. and A. L. Vladu (2017): "Below the zero lower bound: a shadow-rate term structure model for the euro area," Working Paper Series 1991, European Central Bank.

Monfort, A., F. Pegoraro, J.-P. Renne, and G. Roussellet (2017): "Staying at zero with affine processes: An application to term structure modelling," *Journal of Econometrics*, 201, 348–366.

Nelson, C. R. and A. F. Siegel (1987): "Parsimonious Modeling of Yield Curves," *The Journal of Business*, 60, 473–489.

Newey, W. K. and K. D. West (1994): "Automatic Lag Selection in Covariance Matrix Estimation," *The Review of Economic Studies*, 61, 631–653.

Ouerk, S., C. Boucher, and C. Lubochinsky (2020): "Unconventional monetary policy in the Euro Area: Shadow rate and light effets," *Journal of Macroeconomics*, 65, 103219.

Roussellet, G. (2020): "The Term Structure of Macroeconomic Risks at the Zero Lower Bound," SSRN Scholarly Paper ID 2863271, Social Science Research Network, Rochester, NY.

Ullah, W. (2019): "The arbitrage-free generalized Nelson–Siegel term structure model: Does a good in-sample fit imply better out-of-sample forecasts?" *Empirical Economics*.

Vasicek, O. (1977): "An equilibrium characterization of the term structure," *Journal of Financial Economics*, 5, 177–188.

von Borstel, J., S. Eickmeier, and L. Krippner (2016): "The interest rate pass-through in the euro area during the sovereign debt crisis," *Journal of International Money and Finance*, 68, 386–402.

Wu, J. C. and F. D. Xia (2016): "Measuring the Macroeconomic Impact of Monetary Policy at the Zero Lower Bound," *Journal of Money, Credit and Banking*, 48, 253–291.

——— (2020): "Negative interest rate policy and the yield curve," *Journal of Applied Econometrics*, 35, 653–672.

A Smooth Shadow-Rate Dynamic Nelson-Siegel Model for Yields at the Zero Lower Bound

Online Appendix

Daan Opschoor Michel van der Wel

January 27, 2022

Contents

A Arbitrage-free models

Here we discuss the specification and estimation of the arbitrage-free Nelson-Siegel (AFNS) model proposed by Christensen et al. (2011). Moreover, we consider the specification and estimation of the shadow-rate AFNS (B-AFNS) model proposed by Christensen and Rudebusch (2015). Both these models are used as benchmarks throughout the empirical results section.

A.1 Arbitrage-free Nelson-Siegel model

Based on the general framework of Duffie and Kan (1996), Christensen et al. (2011) show that the arbitrage-free bond yield with time to maturity τ at time t can be described as the well-known Nelson and Siegel (1987) factor loading structure given by

$$y_t(\tau) = X_t^1 + \left(\frac{1-e^{-\lambda\tau}}{\lambda\tau}\right)X_t^2 + \left(\frac{1-e^{-\lambda\tau}}{\lambda\tau} - e^{-\lambda\tau}\right)X_t^3 - \frac{A(\tau)}{\tau}, \tag{A.1}$$

where the latent factors X_t^1, X_t^2 and X_t^3 have the interpretation of level, slope and curvature, respectively, and follow the continuous-time process

$$\begin{pmatrix} dX_t^1 \\ dX_t^2 \\ dX_t^3 \end{pmatrix} = - \begin{pmatrix} 0 & 0 & 0 \\ 0 & \lambda & -\lambda \\ 0 & 0 & \lambda \end{pmatrix} \begin{pmatrix} X_t^1 \\ X_t^2 \\ X_t^3 \end{pmatrix} dt + \begin{pmatrix} \sigma_{11} & 0 & 0 \\ \sigma_{21} & \sigma_{22} & 0 \\ \sigma_{31} & \sigma_{32} & \sigma_{33} \end{pmatrix} \begin{pmatrix} dW_t^{1,\mathbb{Q}} \\ dW_t^{2,\mathbb{Q}} \\ dW_t^{3,\mathbb{Q}} \end{pmatrix} \tag{A.2}$$

under the risk-neutral $\mathbb{Q}$-measure where $\lambda > 0$ and $dW_t^{i,\mathbb{Q}}$ is a standard Brownian motion for $i = 1, 2, 3$. Note that this specification already includes the identification that the mean levels of the factors under the $\mathbb{Q}$-measure are zero and that the volatility matrix is lower triangular. The corresponding short rate is defined as $r_t = X_t^1 + X_t^2$.

The yield-adjustment term, $-A(\tau)/\tau$, is given in Christensen et al. (2011) and is a function of the volatility matrix parameters, the loading parameter λ, and the time-to-maturity τ. This term is also the key difference between the yield curve expression of the DNS and AFNS model, that is, setting this term equal to zero in the AFNS model returns the yield curve expression of the DNS model.

The relation between the real-world dynamics under the $\mathbb{P}$-measure and the risk-

neutral dynamics under the $\mathbb{Q}$-measure is given by

$$d\boldsymbol{W}_t^{\mathbb{Q}} = d\boldsymbol{W}_t^{\mathbb{P}} + \boldsymbol{\Gamma}_t dt, \tag{A.3}$$

where $d\boldsymbol{W}_t^u = (dW_t^{1,u}, dW_t^{2,u}, dW_t^{3,u})'$ for $u \in \{\mathbb{P}, \mathbb{Q}\}$ and $\boldsymbol{\Gamma}_t$ is a 3×1 vector representing the risk premium. Christensen et al. (2011) assume the essentially affine risk premium specification of Duffee (2002), that is,

$$\boldsymbol{\Gamma}_t = \begin{pmatrix} \gamma_1^0 \\ \gamma_2^0 \\ \gamma_3^0 \end{pmatrix} + \begin{pmatrix} \gamma_{11}^1 & \gamma_{12}^1 & \gamma_{13}^1 \\ \gamma_{21}^1 & \gamma_{22}^1 & \gamma_{23}^1 \\ \gamma_{31}^1 & \gamma_{32}^1 & \gamma_{33}^1 \end{pmatrix} \begin{pmatrix} X_t^1 \\ X_t^2 \\ X_t^3 \end{pmatrix}, \tag{A.4}$$

such that the real-world dynamics of the latent factors under the $\mathbb{P}$-measure are given by

$$\begin{pmatrix} dX_t^1 \\ dX_t^2 \\ dX_t^3 \end{pmatrix} = \begin{pmatrix} \kappa_{11} & \kappa_{12} & \kappa_{13} \\ \kappa_{21} & \kappa_{22} & \kappa_{23} \\ \kappa_{31} & \kappa_{32} & \kappa_{33} \end{pmatrix} \left[\begin{pmatrix} \theta_1 \\ \theta_2 \\ \theta_3 \end{pmatrix} - \begin{pmatrix} X_t^1 \\ X_t^2 \\ X_t^3 \end{pmatrix} \right] dt + \begin{pmatrix} \sigma_{11} & 0 & 0 \\ \sigma_{21} & \sigma_{22} & 0 \\ \sigma_{31} & \sigma_{32} & \sigma_{33} \end{pmatrix} \begin{pmatrix} dW_t^{1,\mathbb{P}} \\ dW_t^{2,\mathbb{P}} \\ dW_t^{3,\mathbb{P}} \end{pmatrix}, \tag{A.5}$$

where the parameters are allowed to vary freely due to the flexible specification of $\boldsymbol{\Gamma}_t$, while at the same time preserving the $\mathbb{Q}$-dynamics and thus the arbitrage-free yield curve expression.

We follow the estimation procedure of Christensen et al. (2011) where the AFNS model is put in a linear Gaussian state space form such that it can be estimated with the Kalman filter, see subsection C.1. Note that $\boldsymbol{F}$ and $\boldsymbol{Q}$, in the notation of subsection C.1, are obtained via eigensystem decomposition (see Fisher and Gilles, 1996; Caldeira et al., 2016, for further details) and that the constant $\boldsymbol{c}$ in the measurement equation is equal to the yield-adjustment term. Moreover, we assume that the real component of the eigenvalues of the matrix with kappa elements in equation (A.5) are positive to ensure covariance stationarity. The starting values for the maximization of the log-likelihood are based on the two-step approach for the DNS model, but transformed such that they correspond to the AFNS model parameters, after which we initially optimize the log-likelihood using a gradient-based optimization method. Then, based on these parameter values as starting values, the final maximization of the log-likelihood is done using the

Nelder-Mead simplex algorithm, which is also used by Christensen et al. (2011).[1]

A.2 Shadow-rate arbitrage-free Nelson-Siegel model

The three-factor shadow-rate arbitrage-free Nelson-Siegel (B-AFNS) model of Christensen and Rudebusch (2015) defines the short rate as proposed by Black (1995), that is,

$$r_t = \max(r_{LB}, s_t), \tag{A.6}$$

where r_{LB} is the lower bound value and the shadow short rate is given by

$$s_t = X_t^1 + X_t^2, \tag{A.7}$$

where the latent factors (X_t^1, X_t^2, X_t^3) again follow the continues-time process under the risk-neutral $\mathbb{Q}$-measure given in equation (A.2).

Under this specification, Krippner (2012) derives based on a bond option price approach that, for any shadow-rate Gaussian affine term structure model, the zero lower bound (ZLB) forward rate approximation is given by

$$\underline{f}_t(\tau) = r_L + \big(f_t(\tau) - r_L\big)\Phi\left(\frac{f_t(\tau) - r_L}{\omega(\tau)}\right) + \omega(\tau)\phi\left(\frac{f_t(\tau) - r_L}{\omega(\tau)}\right), \tag{A.8}$$

where $f_t(\tau)$ is called the shadow forward rate and $\underline{f}_t(\tau)$ the ZLB forward rate, and $\Phi(\cdot)$ and $\phi(\cdot)$ are the cumulative and probability density functions of a standard normal distribution, respectively. Moreover, $\omega(\tau)$ is related to the risk-neutral conditional variance of the shadow short rate. In particular, Christensen and Rudebusch (2015) show that for a shadow-rate AFNS model

$$\begin{aligned}\omega(\tau)^2 = {} & \sigma_{11}^2\tau + \big(\sigma_{21}^2 + \sigma_{22}^2\big)\left(\frac{1 - e^{-2\lambda\tau}}{2\lambda}\right) \\ & + \big(\sigma_{31}^2 + \sigma_{32}^2 + \sigma_{33}^2\big)\left(\frac{1 - e^{-2\lambda\tau}}{4\lambda} - \frac{1}{2}\tau e^{-2\lambda\tau} - \frac{1}{2}\lambda\tau^2 e^{-2\lambda\tau}\right) \\ & + 2\sigma_{21}\sigma_{22}\left(\frac{1 - e^{-\lambda\tau}}{\lambda}\right) + 2\sigma_{11}\sigma_{31}\left(\frac{1 - e^{-\lambda\tau}}{\lambda} - \tau e^{-\lambda\tau}\right)\end{aligned}$$

[1] In the expanding-window forecasting exercise, we only do the two consecutive numerical optimization steps for the first estimation round, after which we only consider the optimization based on the Nelder-Mead simplex algorithm with as starting values the optimized parameters of the previous round.

$$+ (\sigma_{21}\sigma_{31} + \sigma_{22}\sigma_{32})\left(\frac{1 - e^{-2\lambda\tau}}{2\lambda} - \tau e^{-2\lambda\tau}\right),$$

and that the shadow forward rate is equal to

$$f_t(\tau) = \frac{\mathrm{d}}{\mathrm{d}\tau}\big(\tau y_t(\tau)\big) = X_t^1 + e^{-\lambda\tau}X_t^2 + \lambda\tau e^{-\lambda\tau}X_t^3 - A^f(\tau). \tag{A.9}$$

The forward rate adjustment term, $-A^f(\tau)$, is given in Christensen and Rudebusch (2015) and is also a function of the volatility matrix parameters, the loading parameter λ, and the time-to-maturity τ. Finally, by using this approximation and the standard yield-forward relation, the arbitrage-free ZLB yield with τ time to maturity at time t is given by

$$\underline{y}_t(\tau) = \frac{1}{\tau}\int_0^\tau \left[r_L + \big(f_t(s) - r_L\big)\Phi\left(\frac{f_t(s) - r_L}{\omega(s)}\right) + \omega(s)\phi\left(\frac{f_t(s) - r_L}{\omega(s)}\right)\right] ds. \tag{A.10}$$

Again, the essentially affine risk premium specification of Duffee (2002) given in equation (A.4) is assumed such that the factors have the $\mathbb{P}$-dynamics given in equation (A.5).

We follow the estimation procedure of Christensen and Rudebusch (2015) where the B-AFNS model is put in nonlinear Gaussian state space form such that it can be estimated with the extended Kalman filter (EKF), see subsection C.2. The matrices $\boldsymbol{F}$ and $\boldsymbol{Q}$, in the notation of subsection C.2, can be obtained in similar fashion as for the AFNS model. Furthermore, the derivatives needed for the EKF are given in Krippner (2015), who also proposes to approximate the integral with rectangular increments. We again restrict the real part of the eigenvalues of the matrix with kappa elements given in equation (A.5) to be positive. Lastly, we use similar starting values for the optimization as for the AFNS model and follow the same optimization routine.

B Parameter estimates

Table B.1: Parameter estimates of the DNS model

$\boldsymbol{\Gamma}$			$\boldsymbol{\Sigma}_\eta$			$\boldsymbol{\alpha}$
1.003***	0.009	-0.008	0.114***			-0.002
(0.004)	(0.008)	(0.011)	(0.009)			(0.033)
-0.039***	0.918***	0.071***	-0.055***	0.142***		0.133**
(0.008)	(0.013)	(0.011)	(0.007)	(0.010)		(0.051)
0.056***	0.061***	0.895***	-0.015	-0.041***	0.574***	-0.336***
(0.014)	(0.029)	(0.024)	(0.016)	(0.015)	(0.050)	(0.102)

$\text{diag}(\boldsymbol{\Sigma}_\varepsilon)$								λ
0.036***	0.000	0.008***	0.005***	0.000	0.003***	0.002***	0.007***	0.051***
(0.002)	(0.001)	(0.001)	(0.000)	(0.000)	(0.000)	(0.000)	(0.001)	(0.001)

Notes: This table contains the parameter estimates of the DNS model. The asterisks $*$, $**$, and $***$ indicate significance at the 10%, 5% and 1% level, respectively. The standard errors are given in parentheses.

Table B.2: Parameter estimates of the SB-DNS model

$\boldsymbol{\Gamma}$			$\boldsymbol{\Sigma}_\eta$			$\boldsymbol{\alpha}$
0.999***	-0.004	-0.003*	0.108***			-0.010
(0.001)	(0.007)	(0.002)	(0.008)			(0.032)
-0.025***	0.969***	0.053***	-0.046***	0.198***		0.103*
(0.007)	(0.005)	(0.009)	(0.008)	(0.016)		(0.058)
0.045***	0.007	0.916***	0.036**	-0.112**	0.763***	-0.405***
(0.015)	(0.010)	(0.018)	(0.016)	(0.023)	(0.072)	(0.089)

$\text{diag}(\boldsymbol{\Sigma}_\varepsilon)$								γ	λ
0.032***	0.000**	0.006***	0.003***	0.000***	0.003***	0.002***	0.003***	2.679***	0.062***
(0.002)	(0.000)	(0.000)	(0.000)	(0.000)	(0.000)	(0.000)	(0.001)	(0.206)	(0.001)

Notes: This table contains the parameter estimates of the SB-DNS model. The asterisks $*$, $**$, and $***$ indicate significance at the 10%, 5% and 1% level, respectively. The standard errors are given in parentheses.

Table B.3: Smoothness parameter estimates based on subsets of yield observations

	Short-term yields	**Medium-term yields**	**Long-term yields**
$\hat{\gamma}$	4.124***	2.182***	2.015***
	(0.527)	(0.216)	(0.106)

Notes: This table shows the smoothness parameter estimates based on a subset of yields observations, that is, short-term yields are 3-month to 2-year yields, medium-term yields are 1-year to 5-year yields, and long-term yields are 3-month to 10-year yields. The asterisks $*$, $**$, and $***$ indicate significance at the 10%, 5% and 1% level, respectively. The standard errors are given in parentheses.

C Estimation framework

C.1 Kalman filter based estimation

The general linear Gaussian state space model (see Durbin and Koopman, 2012) can be written as

$$\boldsymbol{y}_t = \boldsymbol{c} + \boldsymbol{Z}\boldsymbol{\xi}_t + \boldsymbol{\varepsilon}_t, \quad \boldsymbol{\varepsilon}_t \sim \mathcal{N}(\boldsymbol{0}, \boldsymbol{H}), \tag{C.1}$$

$$\boldsymbol{\xi}_{t+1} = \boldsymbol{d} + \boldsymbol{F}\boldsymbol{\xi}_t + \boldsymbol{\eta}_t, \quad \boldsymbol{\eta}_t \sim \mathcal{N}(\boldsymbol{0}, \boldsymbol{Q}), \quad t = 1, \ldots, T, \tag{C.2}$$

where equations (C.1) and (C.2) are the measurement and state equation, respectively, $\boldsymbol{y}_t$ is the $N \times 1$ observation vector and $\boldsymbol{\xi}_t$ is the $K \times 1$ state vector with some unobserved factors. Also, some elements of $\boldsymbol{c}$ $(N \times 1)$, $\boldsymbol{Z}$ $(N \times K)$, $\boldsymbol{H}$ $(N \times N)$, $\boldsymbol{d}$ $(K \times 1)$, $\boldsymbol{F}$ $(K \times K)$ and $\boldsymbol{Q}$ $(K \times K)$ are known, while the others are unknown parameters that need to be estimated. Both the DNS and AFNS model fit this representation, see Christensen et al. (2011) for further details.

Given the unknown parameter set Θ, the latent factors in the state vector $\boldsymbol{\xi}_t$ can be recursively obtained via the Kalman filter (KF) (see Durbin and Koopman, 2012). We define the predicted state and its covariance matrix at time t as $\widehat{\boldsymbol{\xi}}_{t|t-1} = \mathrm{E}(\boldsymbol{\xi}_t|\boldsymbol{\mathcal{I}}_{t-1})$ and $\boldsymbol{P}_{t|t-1} = \mathrm{var}(\boldsymbol{\xi}_t|\boldsymbol{\mathcal{I}}_{t-1})$, respectively, where $\boldsymbol{\mathcal{I}}_{t-1} = (\boldsymbol{y}_1', \ldots, \boldsymbol{y}_{t-1}')'$ denotes the information set available at time $t-1$. Moreover, we define the updated state and its covariance matrix at time t as $\widehat{\boldsymbol{\xi}}_{t|t} = \mathrm{E}(\boldsymbol{\xi}_t|\boldsymbol{\mathcal{I}}_t)$ and $\boldsymbol{P}_{t|t} = \mathrm{var}(\boldsymbol{\xi}_t|\boldsymbol{\mathcal{I}}_t)$, respectively. For given values of the predicted state and its uncertainty at time t, we conduct the updating step of the KF to obtain the updated state and its uncertainty, that is,

$$\widehat{\boldsymbol{\xi}}_{t|t} = \widehat{\boldsymbol{\xi}}_{t|t-1} + \boldsymbol{P}_{t|t-1}\boldsymbol{Z}'\boldsymbol{V}_t^{-1}\boldsymbol{v}_t, \tag{C.3}$$

$$\boldsymbol{P}_{t|t} = \boldsymbol{P}_{t|t-1} - \boldsymbol{P}_{t|t-1}\boldsymbol{Z}'\boldsymbol{V}_t^{-1}\boldsymbol{Z}\boldsymbol{P}_{t|t-1}, \tag{C.4}$$

where $\boldsymbol{v}_t = \boldsymbol{y}_t - \boldsymbol{c} - \boldsymbol{Z}\widehat{\boldsymbol{\xi}}_{t|t-1}$ is the prediction error vector and $\boldsymbol{V}_t = \boldsymbol{Z}\boldsymbol{P}_{t|t-1}\boldsymbol{Z}' + \boldsymbol{H}$ is the prediction error covariance matrix. Next, for given values of the updated state and its uncertainty at time t, we conduct the prediction step of the KF to obtain the predicted state and its uncertainty, that is,

$$\widehat{\boldsymbol{\xi}}_{t+1|t} = \boldsymbol{d} + \boldsymbol{F}\widehat{\boldsymbol{\xi}}_{t|t}, \tag{C.5}$$

$$\boldsymbol{P}_{t+1|t} = \boldsymbol{F}\boldsymbol{P}_{t|t}\boldsymbol{F}' + \boldsymbol{Q}. \tag{C.6}$$

A formal derivation of the KF can be found in Durbin and Koopman (2012). We assume that $\boldsymbol{\xi}_0 \sim \mathcal{N}(\boldsymbol{\mu}, \boldsymbol{W})$ such that $\widehat{\boldsymbol{\xi}}_{0|0} = \boldsymbol{\mu}$ and $\boldsymbol{P}_{0|0} = \boldsymbol{W}$, where $\boldsymbol{\mu} = (\boldsymbol{I}_r - \boldsymbol{F})^{-1}\boldsymbol{d}$ is the unconditional mean and $\boldsymbol{W}$ is the unconditional covariance matrix for which it holds that $\boldsymbol{W} - \boldsymbol{F}\boldsymbol{W}\boldsymbol{F}' = \boldsymbol{Q}$, see Hamilton (1994, section 2.2). Finally, based on the initialization and the recursions of the KF in equations (C.3)-(C.6) we are able to obtain the latent factor estimates $\widehat{\boldsymbol{\xi}}_{t|t-1}$ and the covariance matrices $\boldsymbol{P}_{t|t-1}$ of these estimates for $t = 1, \ldots, T$.

Given the latent factor estimates, we can evaluate the log-likelihood function based on the prediction error decomposition given by

$$\ell(\boldsymbol{y}_1, \ldots, \boldsymbol{y}_T; \boldsymbol{\Theta}) = -\frac{nT}{2}\log 2\pi - \frac{1}{2}\sum_{t=1}^{T}\Big(\log|\boldsymbol{V}_t| + \boldsymbol{v}_t'\boldsymbol{V}_t^{-1}\boldsymbol{v}_t\Big), \tag{C.7}$$

where $\boldsymbol{v}_t$ and $\boldsymbol{V}_t$ are the prediction error vector and covariance matrix, respectively, and are given by the KF. We numerically maximize the log-likelihood with respect to $\boldsymbol{\Theta}$ to obtain the maximum likelihood parameter estimates.

C.2 Extended Kalman filter based estimation

The general nonlinear Gaussian state space model (see Durbin and Koopman, 2012) can be written as

$$\boldsymbol{y}_t = \boldsymbol{Z}(\boldsymbol{\xi}_t) + \boldsymbol{\varepsilon}_t, \qquad \boldsymbol{\varepsilon}_t \sim \mathcal{N}(\boldsymbol{0}, \boldsymbol{H}), \tag{C.8}$$

$$\boldsymbol{\xi}_{t+1} = \boldsymbol{d} + \boldsymbol{F}\boldsymbol{\xi}_t + \boldsymbol{\eta}_t, \quad \boldsymbol{\eta}_t \sim \mathcal{N}(\boldsymbol{0}, \boldsymbol{Q}), \quad t = 1, \ldots, T, \tag{C.9}$$

where equations (C.8) and (C.9) are the nonlinear measurement and linear state equation, respectively, and $\boldsymbol{Z}(\boldsymbol{\xi}_t)$ is a differentiable function of $\boldsymbol{\xi}_t$. Both the (smooth) shadow-rate models as well as the models with time-varying factor loadings fit this nonlinear state space representation. The expressions of $\boldsymbol{\xi}_t$ and $\boldsymbol{Z}(\boldsymbol{\xi}_t)$ for each specific model are given in subsection C.3. The parameter set Θ is the same as for the linear Gaussian state space model, except that we could also include the lower bound r_{LB} and/or the smoothness parameter γ as additional unknown parameters in case we do not prefix them.

Given the parameter set Θ, the latent factors in the state vector $\boldsymbol{\xi}_t$ can be recursively obtained via the extended Kalman filter (EKF). In order to implement the EKF, we first need to linearize the nonlinear meausrement equation (C.8) by applying a first-order Taylor series expansion of $\boldsymbol{Z}(\boldsymbol{\xi}_t)$ at $\boldsymbol{\xi}_t = \widehat{\boldsymbol{\xi}}_{t|t-1}$, that is,

$$\begin{aligned} \boldsymbol{y}_t &= \boldsymbol{Z}(\boldsymbol{\xi}_t) + \boldsymbol{\varepsilon}_t \\ &= \boldsymbol{Z}(\widehat{\boldsymbol{\xi}}_{t|t-1}) + \dot{\boldsymbol{Z}}_t(\boldsymbol{\xi}_t - \widehat{\boldsymbol{\xi}}_{t|t-1}) + \boldsymbol{\varepsilon}_t \\ &= \boldsymbol{c}_t + \dot{\boldsymbol{Z}}_t\boldsymbol{\xi}_t + \boldsymbol{\varepsilon}_t, \end{aligned} \tag{C.10}$$

where

$$\dot{\boldsymbol{Z}}_t = \left.\frac{\partial \boldsymbol{Z}(\boldsymbol{\xi}_t)}{\partial \boldsymbol{\xi}_t'}\right|_{\boldsymbol{\xi}_t = \widehat{\boldsymbol{\xi}}_{t|t-1}} \quad \text{and} \quad \boldsymbol{c}_t = \boldsymbol{Z}(\widehat{\boldsymbol{\xi}}_{t|t-1}) - \dot{\boldsymbol{Z}}_t\widehat{\boldsymbol{\xi}}_{t|t-1}. \tag{C.11}$$

The expression of $\dot{\boldsymbol{Z}}_t$ for each specific model is given in Appendix C.3. For given values of the predicted state and its uncertainty at time t, we are able to conduct the updating step of the EKF to obtain the updated state and its uncertainty, that is,

$$\widehat{\boldsymbol{\xi}}_{t|t} = \widehat{\boldsymbol{\xi}}_{t|t-1} + \boldsymbol{P}_{t|t-1}\dot{\boldsymbol{Z}}_t'\boldsymbol{V}_t^{-1}\boldsymbol{v}_t, \tag{C.12}$$

$$\boldsymbol{P}_{t|t} = \boldsymbol{P}_{t|t-1} - \boldsymbol{P}_{t|t-1}\dot{\boldsymbol{Z}}_t'\boldsymbol{V}_t^{-1}\dot{\boldsymbol{Z}}_t\boldsymbol{P}_{t|t-1}, \tag{C.13}$$

where $\boldsymbol{v}_t = \boldsymbol{y}_t - \boldsymbol{Z}(\widehat{\boldsymbol{\xi}}_{t|t-1})$ is the prediction error vector and $\boldsymbol{V}_t = \dot{\boldsymbol{Z}}_t\boldsymbol{P}_{t|t-1}\dot{\boldsymbol{Z}}_t' + \boldsymbol{H}$ is the prediction error covariance matrix. Next, for given values of the updated state and its uncertainty at time t, we conduct the prediction step of the EKF, which is in this case the same as for the KF given by equations (C.5)-(C.6), to obtain the predicted state and its uncertainty. A formal derivation of the EKF can be found in Durbin and Koopman (2012). We again assume the initialization $\boldsymbol{\xi}_0 \sim \mathcal{N}(\boldsymbol{\mu}, \boldsymbol{W})$ such that the recursions of the EKF in equations (C.12)-(C.13) and (C.5)-(C.6) provide us with the latent factor estimates $\widehat{\boldsymbol{\xi}}_{t|t-1}$ and the covariance matrix $\boldsymbol{P}_{t|t-1}$ of these estimates for $t = 1, \ldots, T$.

Similarly as for the KF based estimation of the linear Gaussian state space model, we estimate the unknown parameters in $\boldsymbol{\Theta}$ by means of maximizing the log-likelihood given by equation (C.7) with numerical optimization, where $\boldsymbol{v}_t$ and $\boldsymbol{V}_t$ are now obtained via the EKF.

C.3 Derivatives for extended Kalman filter

C.3.1 DNS-TVL

In the context of the DNS-TVL model, we have

$$\boldsymbol{Z}(\boldsymbol{\xi}_t) = \boldsymbol{\Lambda}(\lambda_t)\boldsymbol{\beta}_t, \tag{C.14}$$

where $\boldsymbol{\xi}_t = (\boldsymbol{\beta}_t{}', \lambda_t)'$. The derivative of $\boldsymbol{Z}(\boldsymbol{\xi}_t)$ with respect to $\boldsymbol{\xi}_t'$ is given by

$$\frac{\partial \boldsymbol{Z}(\boldsymbol{\xi}_t)}{\partial \boldsymbol{\xi}_t'} = \begin{pmatrix} \frac{\partial \boldsymbol{\Lambda}(\lambda_t)\boldsymbol{\beta}_t}{\partial \boldsymbol{\beta}_t{}'} & \frac{\partial \boldsymbol{\Lambda}(\lambda_t)\boldsymbol{\beta}_t}{\partial \lambda_t} \end{pmatrix} = \begin{pmatrix} \boldsymbol{\Lambda}(\lambda_t) & \boldsymbol{U}(\lambda_t)\boldsymbol{\beta}_t \end{pmatrix}, \tag{C.15}$$

where

$$\boldsymbol{U}(\lambda_t) = \begin{pmatrix} 0 & u_1(\tau_1, \lambda_t) & u_2(\tau_1, \lambda_t) \\ \vdots & \vdots & \vdots \\ 0 & u_1(\tau_N, \lambda_t) & u_2(\tau_N, \lambda_t) \end{pmatrix}, \tag{C.16}$$

with

$$u_1(\tau_i, \lambda_t) = \frac{\partial}{\partial \lambda_t}\left(\frac{1 - e^{-\lambda_t \tau_i}}{\lambda_t \tau_i}\right) = \frac{(1 + \tau_i \lambda_t)e^{-\lambda_t \tau_i} - 1}{\lambda_t^2 \tau_i}, \tag{C.17}$$

and

$$u_2(\tau_i, \lambda_t) = \frac{\partial}{\partial \lambda_t}\left(\frac{1 - e^{-\lambda_t \tau_i}}{\lambda_t \tau_i} - e^{-\lambda_t \tau_i}\right) = \frac{(1 + \tau_i \lambda_t)e^{-\lambda_t \tau_i} - 1}{\lambda_t^2 \tau_i} + \tau_i e^{-\lambda_t \tau_i}, \tag{C.18}$$

for $i = 1, \ldots, N$.

C.3.2 B-DNS

In the context of the B-DNS model, we have

$$\boldsymbol{Z}(\boldsymbol{\xi}_t) = r_{LB}\boldsymbol{\iota} + (\boldsymbol{\Lambda}(\lambda)\boldsymbol{\beta}_t - r_{LB}\boldsymbol{\iota}) \odot \boldsymbol{L}_t, \tag{C.19}$$

where $\boldsymbol{\xi}_t = \boldsymbol{\beta}_t$, $\odot$ is the Hadamard product, $\boldsymbol{\iota}$ denotes an $N \times 1$ vector with ones, $\boldsymbol{L}_t = (L_{1t}, \ldots, L_{Nt})'$ and $L_{it} = \mathbb{I}(y_t(\tau_i) - r_{LB} > 0)$ with $\mathbb{I}(A)$ being an indicator function that is equal to 1 if event A is true and zero otherwise. The derivative of $\boldsymbol{Z}(\boldsymbol{\xi}_t)$ with

respect to $\boldsymbol{\xi}_t'$ is given by

$$\frac{\partial \boldsymbol{Z}(\boldsymbol{\xi}_t)}{\partial \boldsymbol{\xi}_t'} = \boldsymbol{L}_t \odot \boldsymbol{\Lambda}(\lambda). \tag{C.20}$$

C.3.3 SB-DNS

In the context of the SB-DNS model, we have

$$\boldsymbol{Z}(\boldsymbol{\xi}_t) = r_{LB}\boldsymbol{\iota} + (\boldsymbol{\Lambda}(\lambda)\boldsymbol{\beta}_t - r_{LB}\boldsymbol{\iota}) \odot \boldsymbol{F}_t + \gamma \boldsymbol{f}_t, \tag{C.21}$$

where $\boldsymbol{\xi}_t = \boldsymbol{\beta}_t$, $\boldsymbol{F}_t = (F_{1t}, \ldots, F_{Nt})'$ with $F_{it} = \Phi\big((y_t(\tau_i) - r_{LB})/\gamma\big)$ and $\boldsymbol{f}_t = (f_{1t}, \ldots, f_{Nt})'$ with $f_{it} = \phi\big((y_t(\tau_i) - r_{LB})/\gamma\big)$. The derivative of $\boldsymbol{Z}(\boldsymbol{\xi}_t)$ with respect to $\boldsymbol{\xi}_t'$ is given by

$$\frac{\partial \boldsymbol{Z}(\boldsymbol{\xi}_t)}{\partial \boldsymbol{\xi}_t'} = \boldsymbol{F}_t \odot \boldsymbol{\Lambda}(\lambda). \tag{C.22}$$

C.3.4 SB-DNS-TVL

In the context of the SB-DNS-TVL model, we have

$$\boldsymbol{Z}(\boldsymbol{\xi}_t) = r_{LB}\boldsymbol{\iota} + (\boldsymbol{\Lambda}(\lambda_t)\boldsymbol{\beta}_t - r_{LB}\boldsymbol{\iota}) \odot \boldsymbol{F}_t + \gamma \boldsymbol{f}_t, \tag{C.23}$$

where $\boldsymbol{\xi}_t = (\boldsymbol{\beta}_t{}', \lambda_t)'$. The derivative of $\boldsymbol{Z}(\boldsymbol{\xi}_t)$ with respect to $\boldsymbol{\xi}_t'$ is given by

$$\frac{\partial \boldsymbol{Z}(\boldsymbol{\xi}_t)}{\partial \boldsymbol{\xi}_t'} = \boldsymbol{F}_t \odot \Big(\boldsymbol{\Lambda}(\lambda_t) \quad \boldsymbol{U}(\lambda_t)\boldsymbol{\beta}_t\Big). \tag{C.24}$$

D Nonzero lower bound analysis

D.1 In-sample fit

Table D.1: Lower bound estimate, log-likelihood and information criteria of shadow rate models

	$\hat{r}_{LB}$	$\hat{\gamma}$	Log-likelihood	$\#\Theta$	AIC	BIC	LR-test	
							Statistic	p-value
SB-DNS	0.044 (0.008)	2.532 (0.183)	3091.3	29	-13.0	-12.8	21.3	0.000
SB-DNS-TVL	0.011 (0.018)	4.296 (0.836)	3251.7	40	-13.7	-13.3	1.4	0.230
B-AFNS	0.072 (0.007)		2632.1	28	-11.1	-10.8	77.8	0.000

Notes: This table contains the lower bound estimates, log-likelihood values, Akaike information criteria (AIC), Bayesian information criteria (BIC) and the likelihood ratio (LR) test statistics and corresponding p-values across shadow-rate models. The LR tests consider the models with fixed lower bound specification of 0% given in Table 2 as null model.

Table D.2: Relative in-sample fit of shadow-rate models with estimated lower bound

Rel. RMSE	Maturities (in months)								Total
	3	6	12	24	36	60	84	120	
Panel A: Total period (December 1981 - October 2020)									
SB-DNS	1.00	1.10	0.99	1.00	0.99	1.00	1.01	0.94	1.00
SB-DNS-TVL	1.00	1.01	1.00	1.00	0.99	1.00	1.00	0.98	1.00
B-AFNS	1.01	1.07	1.00	0.97	1.12	0.98	0.99	0.98	1.00
Panel B: Pre-ZLB period (December 1981 - October 2008)									
SB-DNS	1.00	1.07	1.00	1.01	0.97	1.00	1.02	0.96	1.00
SB-DNS-TVL	1.00	1.00	1.00	1.00	0.99	1.00	1.00	0.99	1.00
B-AFNS	1.01	0.90	1.00	0.97	1.10	0.99	0.98	1.00	1.00
Panel C: ZLB period (November 2008 - December 2015)									
SB-DNS	1.12	2.19	0.85	1.00	1.00	1.26	0.80	1.23	1.05
SB-DNS-TVL	0.98	1.28	0.82	0.73	1.16	0.73	1.03	0.69	0.91
B-AFNS	1.11	1.13	0.95	0.87	1.12	0.82	1.01	0.90	0.99

Notes: This table contains the relative Root Mean Squared Errors (RMSE) across maturities of shadow-rate models with a fixed lower bound specification of 0% compared to an estimated lower bound over three sample periods. We discard the first three observations from this calculation to make the results robust to the unconditional initialization. The shaded cells indicate a relative RMSE that is smaller than 1, which implies a better fit of the shadow-rate model with an estimated lower bound relative to the fixed lower bound specification of 0% given in Tables 3.

Table D.3: In-sample fit of SB-DNS models with various lower bound values

RMSE	r_{LB}	Maturities (in months)								Total
		3	**6**	**12**	**24**	**36**	**60**	**84**	**120**	
Panel A: Total period (December 1981 - October 2020)										
SB-DNS	0.00%	17.7	1.1	8.0	5.8	0.8	5.3	4.1	4.0	7.7
	0.05%	17.6	1.5	7.9	5.7	0.9	5.3	4.2	3.7	7.6
	0.10%	17.5	2.7	7.4	5.5	1.0	5.2	4.2	3.4	7.6
	0.15%	17.8	4.5	6.9	5.2	1.4	5.2	4.2	3.2	7.7
	0.20%	18.4	6.3	7.0	5.0	1.9	5.1	4.2	2.9	8.0
Panel B: Pre-ZLB period (December 1981 - October 2008)										
SB-DNS	0.00%	20.5	0.3	9.0	6.4	0.4	5.5	4.3	4.0	8.7
	0.05%	20.3	0.6	8.9	6.4	0.5	5.5	4.4	3.8	8.6
	0.10%	19.8	1.9	8.3	6.1	0.7	5.5	4.5	3.6	8.4
	0.15%	19.6	3.5	7.6	5.8	1.1	5.4	4.5	3.4	8.3
	0.20%	19.7	4.7	7.1	5.5	1.6	5.4	4.5	3.2	8.3
Panel C: ZLB period (November 2008 - December 2015)										
SB-DNS	0.00%	8.3	1.3	4.8	4.2	1.1	5.2	4.4	4.6	4.7
	0.05%	8.7	2.1	4.5	4.1	1.3	5.3	4.4	4.1	4.8
	0.10%	10.7	4.3	4.2	3.7	1.3	5.2	4.3	3.5	5.3
	0.15%	13.5	7.3	5.1	3.2	1.5	5.0	4.1	3.0	6.4
	0.20%	16.8	10.7	7.1	3.0	1.8	4.8	3.9	2.7	7.9

Notes: This table contains the Root Mean Squared Errors (RMSE) across maturities of shadow-rate models with a fixed lower bound specification of 0% and smoothness parameter $\gamma = 1$ compared to various nonzero lower bound values over three sample periods. We discard the first three observations from this calculation to make the results robust to the initial conditions. The shaded cells indicate a RMSE that is smaller than the SB-DNS model with a lower bound of 0%, which implies a better fit of the shadow-rate model with a nonzero lower bound value relative to a fixed lower bound specification of 0%.

D.2 Forecasting results

Table D.4: Forecasting performance of SB-DNS models with various lower bound values

RMSFE	r_{LB}	Maturities (in months)							
		3	**6**	**12**	**24**	**36**	**60**	**84**	**120**
Panel A: One-month-ahead forecasts (h = 1)									
SB-DNS	0.00%	22.6	18.4	19.5	23.6	25.6	26.9	27.1	26.0
	0.05%	23.3	18.4	19.2	23.5	25.7	27.0	27.2	26.0
	0.10%	23.9	18.5	19.1	23.5	25.7	27.0	27.1	25.9
	0.15%	24.5	18.8	19.0	23.4	25.7	27.1	27.2	25.8
	0.20%	25.7	19.5	19.2	23.2	25.6	27.2	27.1	25.9
Panel B: Six-month-ahead forecasts (h = 6)									
SB-DNS	0.00%	62.7	65.3	67.2	70.8	72.6	71.1	67.7	63.0
	0.05%	64.7	66.0	68.0	72.3	74.3	72.8	69.1	63.8
	0.10%	66.5	67.2	69.0	73.2	75.1	72.9	69.0	63.5
	0.15%	66.6	66.9	68.5	72.7	74.6	72.4	68.4	62.6
	0.20%	67.2	66.8	67.8	71.7	73.7	72.5	69.0	64.2
Panel C: One-year-ahead forecasts (h = 12)									
SB-DNS	0.00%	107.1	109.4	109.2	107.8	105.8	98.7	92.4	84.8
	0.05%	112.9	114.0	113.7	113.0	111.2	103.2	96.0	87.2
	0.10%	117.5	117.9	117.5	116.6	114.3	105.2	97.5	88.4
	0.15%	117.5	117.5	117.1	116.3	113.8	103.9	95.6	85.9
	0.20%	116.3	115.8	114.8	113.4	111.2	103.5	96.9	89.6
Panel D: Two-year-ahead forecasts (h = 24)									
SB-DNS	0.00%	170.1	170.3	165.2	155.8	149.9	137.7	125.8	111.5
	0.05%	188.9	188.0	183.1	174.0	167.4	152.2	138.2	122.3
	0.10%	202.1	200.8	195.8	185.9	177.9	160.7	145.5	128.6
	0.15%	204.5	203.0	198.0	188.0	179.1	159.5	143.3	126.7
	0.20%	198.1	196.2	190.6	180.0	172.0	156.7	144.1	132.2

Notes: This table contains the Root Mean Squared Forecast Errors (RMSFE) across maturities and horizons of SB-DNS models with a fixed lower bound specification of 0% and smoothness parameter $\gamma = 1$ compared to various nonzero lower bound values over three sample periods. We consider expanding-window estimation with the initial sample from September 1981 to Augustus 2001 (240 observations) resulting in 230 one-month-ahead forecasts, 225 six-month-ahead forecasts, 219 one-year-ahead forecasts and 207 two-year-ahead forecasts to compute the RMSFEs. The shaded cells indicate a RMSFE that is smaller than the one of the SB-DNS model with a lower bound of 0%, which a better out-of-sample performance of the shadow-rate model with a nonzero lower bound value relative to a fixed lower bound specification.

E Alternative shadow short rate estimates

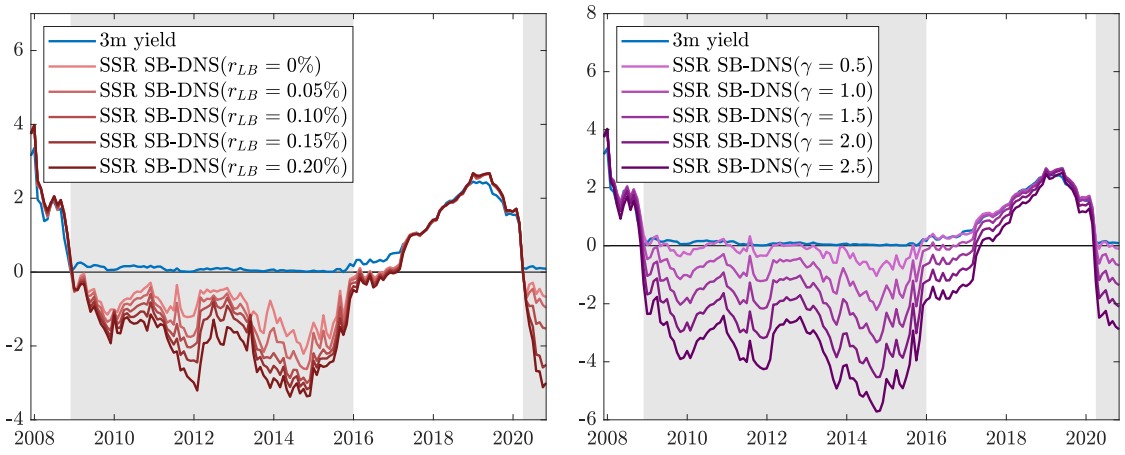

(a) Lower bound analysis with $\gamma = 1$ **(b)** Smoothness analysis with $r_{LB} = 0\%$

Figure E.1: Robustness analysis of shadow short rate estimates towards lower bound value and smoothness parameter

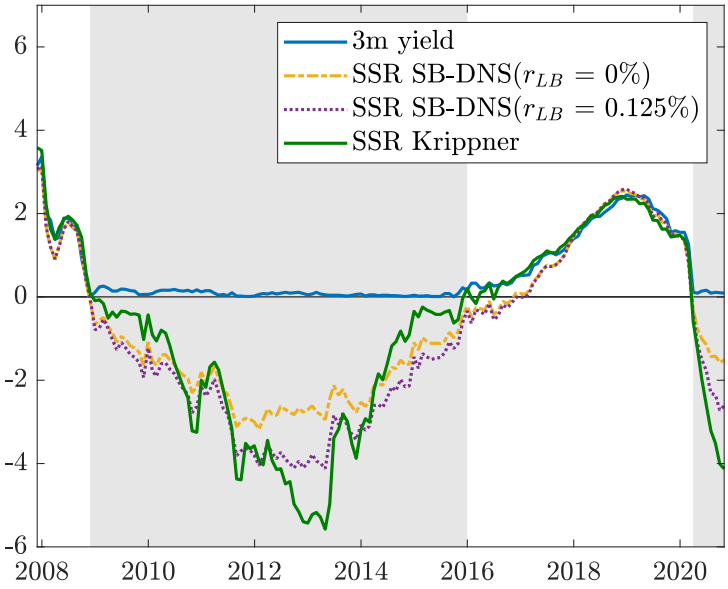

Figure E.2: Shadow short rate estimates based on two-factor models with $\gamma = 1$

F Smoothness analysis

F.1 In-sample fit

Table F.1: In-sample fit of SB-DNS models with various smoothness parameter values

RMSE	γ	Maturities (in months)								Total
		3	6	12	24	36	60	84	120	
Panel A: Total period (December 1981 - October 2020)										
B-DNS		18.1	0.0	8.7	6.8	0.0	5.6	3.0	7.0	8.2
SB-DNS	0.5	17.9	0.8	8.3	6.1	0.4	5.5	3.6	5.6	7.9
	1.0	17.7	1.1	8.0	5.8	0.8	5.3	4.1	4.0	7.7
	1.5	17.6	1.4	7.8	5.5	1.1	5.1	4.1	3.7	7.6
	2.0	17.4	1.6	7.6	5.3	1.4	5.0	4.1	3.7	7.5
	2.5	17.4	1.7	7.5	5.2	1.6	5.0	4.1	3.8	7.5
	3.0	17.4	1.8	7.5	5.0	1.7	5.0	4.1	3.9	7.5
	3.5	17.3	1.9	7.4	4.9	1.9	5.0	4.0	4.0	7.5
	4.0	17.3	2.0	7.4	4.9	2.0	5.0	4.0	4.1	7.5
Panel B: Pre-ZLB period (December 1981 - October 2008)										
B-DNS		20.7	0.0	9.2	6.8	0.0	5.8	3.1	6.3	9.0
SB-DNS	0.5	20.6	0.0	9.2	6.7	0.2	5.7	3.7	5.2	8.9
	1.0	20.5	0.3	9.0	6.4	0.4	5.5	4.3	4.0	8.7
	1.5	20.2	0.6	8.7	6.1	0.8	5.3	4.4	3.8	8.6
	2.0	20.1	0.8	8.5	5.9	1.1	5.2	4.4	3.8	8.5
	2.5	20.0	0.9	8.4	5.7	1.3	5.2	4.3	3.9	8.4
	3.0	19.9	1.1	8.3	5.6	1.5	5.2	4.2	3.9	8.4
	3.5	19.9	1.2	8.2	5.4	1.7	5.2	4.2	4.0	8.4
	4.0	19.9	1.3	8.2	5.3	1.8	5.2	4.1	4.1	8.3
Panel C: ZLB period (November 2008 - December 2015)										
B-DNS		10.9	0.0	8.6	7.9	0.0	5.9	3.4	10.7	7.2
SB-DNS	0.5	8.9	1.3	5.5	5.3	0.6	5.9	4.2	7.8	5.6
	1.0	8.3	1.3	4.8	4.2	1.1	5.2	4.4	4.6	4.7
	1.5	8.2	1.6	4.6	3.7	1.5	4.9	4.3	4.0	4.5
	2.0	8.2	1.9	4.5	3.5	1.7	4.7	4.2	4.0	4.5
	2.5	8.1	2.0	4.4	3.4	1.9	4.7	4.4	4.0	4.5
	3.0	8.1	2.2	4.4	3.4	2.1	4.6	4.4	4.2	4.5
	3.5	8.1	2.3	4.4	3.4	2.3	4.6	4.4	4.4	4.6
	4.0	8.2	2.4	4.4	3.4	2.4	4.6	4.4	4.5	4.6

Notes: This table contains the Root Mean Squared Errors (RMSE) across maturities of the B-DNS model with a fixed lower bound specification of 0% compared to SB-DNS models with various nonzero smoothness parameters over three sample periods. We discard the first three observations from this calculation to make the results robust to the initial conditions. The shaded cells indicate a RMSE that is smaller than the one of the B-DNS, which implies a better fit of the SB-DNS model with $\gamma > 0$ relative to a B-DNS model.

F.2 Forecasting results

Table F.2: Forecasting performance of SB-DNS models with various smoothness parameter values

RMSFE	γ	Maturities (in months)							
		3	**6**	**12**	**24**	**36**	**60**	**84**	**120**
Panel A: One-month-ahead forecasts (h = 1)									
B-DNS		25.4	19.1	19.8	23.7	25.7	27.4	27.2	26.9
SB-DNS	0.5	23.2	18.3	19.6	24.0	25.8	27.2	27.2	26.5
	1.0	22.6	18.4	19.5	23.6	25.6	26.9	27.1	26.0
	1.5	23.7	18.5	19.1	23.5	25.7	27.0	27.1	25.8
	2.0	23.9	18.7	19.1	23.4	25.8	27.2	27.3	26.0
	2.5	24.0	18.8	19.1	23.4	25.9	27.3	27.4	26.1
	3.0	23.7	19.0	19.2	23.4	25.8	27.2	27.3	26.2
	3.5	23.9	19.1	19.1	23.3	25.9	27.4	27.3	26.3
	4.0	24.1	19.2	19.2	23.3	26.0	27.4	27.3	26.5
Panel B: Six-month-ahead forecasts (h = 6)									
B-DNS		70.8	68.9	68.7	72.4	74.8	74.0	70.7	67.4
SB-DNS	0.5	66.7	68.2	70.7	75.3	76.9	74.2	70.3	65.5
	1.0	62.7	65.3	67.2	70.8	72.6	71.1	67.7	63.0
	1.5	66.8	67.5	69.4	73.7	75.4	72.9	68.9	63.4
	2.0	67.1	67.7	69.4	73.6	75.4	73.7	70.1	64.7
	2.5	66.9	67.5	69.0	73.1	75.2	74.0	70.7	65.9
	3.0	65.2	66.3	67.5	71.2	73.4	72.7	69.7	65.4
	3.5	66.1	66.9	67.8	71.5	73.9	73.5	70.5	66.5
	4.0	66.5	67.0	67.7	71.1	73.5	73.4	70.6	67.7
Panel C: One-year-ahead forecasts (h = 12)									
B-DNS		117.0	115.1	113.2	112.2	111.1	105.0	99.2	94.1
SB-DNS	0.5	119.6	120.6	121.1	120.8	118.1	107.7	99.4	90.6
	1.0	107.1	109.4	109.2	107.8	105.8	98.7	92.4	84.8
	1.5	118.2	118.5	118.2	117.5	114.8	105.0	97.2	88.3
	2.0	118.1	118.4	117.9	116.9	114.6	105.9	98.6	89.9
	2.5	117.0	117.2	116.7	115.9	114.1	106.8	100.3	92.5
	3.0	110.7	111.5	110.7	109.7	108.6	103.0	97.6	91.3
	3.5	111.6	112.1	111.0	110.2	109.4	104.6	99.5	94.0
	4.0	111.7	111.8	110.3	109.0	108.3	104.5	100.5	97.1
Panel D: Two-year-ahead forecasts (h = 24)									
B-DNS		189.0	186.5	180.7	171.0	163.8	149.8	138.2	128.7
SB-DNS	0.5	203.3	202.2	197.8	189.2	181.7	163.6	147.5	130.8
	1.0	170.1	170.3	165.2	155.8	149.9	137.7	125.8	111.5
	1.5	204.6	203.5	198.7	189.0	180.7	163.3	148.5	132.0
	2.0	201.1	199.9	195.1	185.3	177.0	159.8	145.5	130.5
	2.5	196.6	195.7	191.2	182.6	175.9	161.6	149.2	136.0
	3.0	175.9	175.6	171.4	164.1	159.7	149.7	140.1	129.5
	3.5	175.0	174.7	170.6	163.9	160.4	152.2	143.5	134.2
	4.0	172.2	171.2	166.1	158.5	155.4	150.0	144.1	138.9

Notes: This table contains the Root Mean Squared Forecast Errors (RMSFE) across maturities and horizons of the B-DNS model with a fixed lower bound specification of 0% compared to SB-DNS models with various nonzero smoothness parameters over three sample periods. We consider expanding-window estimation with the initial sample from September 1981 to Augustus 2001 (240 observations) resulting in 230 one-month-ahead forecasts, 225 six-month-ahead forecasts, 219 one-year-ahead forecasts and 207 two-year-ahead forecasts to compute the RMSFEs. The shaded cells indicate a RMSFE that is smaller than the one of the B-DNS model, which implies a better out-of-sample performance of the SB-DNS model with $\gamma > 0$ relative to the B-DNS model.

G Additional forecasting results

G.1 Forecasting results for rolling-window estimation

Table G.1: Out-of-sample performance based on rolling-window estimation

RMSFE	**Maturities (in months)**							
	3	**6**	**12**	**24**	**36**	**60**	**84**	**120**
Panel A: One-month-ahead forecasts (h = 1)								
RW	**20.5**	19.3	19.4	**22.7**	**24.7**	**26.3**	**26.4**	**25.5**
DNS	25.5	19.0	19.0	23.6	26.5	28.0	27.7	28.1
DNS-TVL	23.8	18.6	**18.7**	23.5	26.9	27.7	27.5	26.5
B-DNS	24.4	**18.6**	19.0	23.6	26.3	27.6	27.5	27.9
SB-DNS	24.2	18.8	18.7	23.3	26.1	27.4	27.5	26.4
SB-DNS-TVL	23.8	18.9	19.0	23.9	27.3	28.4	28.1	27.1
AFNS	32.4	31.3	31.7	31.2	30.2	28.0	28.0	28.3
B-AFNS	24.2	21.9	23.0	25.4	26.4	26.5	27.0	26.6
Panel B: Six-month-ahead forecasts (h = 6)								
RW	66.8	66.7	**65.3**	**66.1**	**67.3**	**65.8**	**63.5**	**60.0**
DNS	71.3	69.5	70.5	76.3	80.3	79.7	75.9	73.1
DNS-TVL	71.4	70.3	73.7	80.6	85.2	83.0	77.6	72.8
B-DNS	**65.7**	**65.2**	66.6	72.5	76.3	75.7	72.5	69.4
SB-DNS	65.9	65.7	66.8	71.7	74.8	73.7	70.2	65.4
SB-DNS-TVL	70.2	70.0	73.5	80.9	85.8	84.1	78.9	73.3
AFNS	111.0	109.9	106.5	99.1	91.4	76.9	69.8	63.4
B-AFNS	79.9	80.5	81.1	80.5	77.6	69.9	65.7	61.0
Panel C: One-year-ahead forecasts (h = 12)								
RW	116.5	115.1	**109.6**	**101.4**	**95.9**	**86.8**	**81.4**	75.5
DNS	121.6	119.9	119.7	121.7	122.5	117.2	110.9	106.4
DNS-TVL	123.6	123.2	127.1	131.8	133.6	126.2	116.6	108.5
B-DNS	**111.5**	**110.9**	110.9	112.4	113.0	107.6	101.9	96.8
SB-DNS	114.2	113.9	113.2	113.0	112.0	104.9	98.4	91.5
SB-DNS-TVL	120.5	121.2	125.4	130.5	132.5	125.3	115.9	107.1
AFNS	146.0	143.9	139.7	129.2	117.6	96.1	86.2	77.7
B-AFNS	123.8	123.2	122.2	116.3	107.8	90.3	82.6	**75.0**
Panel D: Two-year-ahead forecasts (h = 24)								
RW	191.4	190.9	181.1	161.6	146.8	124.4	110.4	97.5
DNS	198.4	195.2	191.4	185.5	181.4	169.8	159.0	151.0
DNS-TVL	205.2	203.3	203.3	201.5	198.3	183.9	168.9	155.7
B-DNS	178.5	175.9	171.4	164.5	160.3	149.3	138.9	129.4
SB-DNS	188.9	186.7	181.8	173.1	166.8	152.6	140.5	129.2
SB-DNS-TVL	198.3	198.3	200.1	199.4	197.0	183.8	169.6	156.5
AFNS	**176.2**	**172.6**	**166.8**	**154.0**	**142.1**	**120.5**	108.7	97.7
B-AFNS	185.1	181.4	176.0	163.1	149.5	123.6	**108.4**	**93.8**

Notes: This table contains the Root Mean Squared Forecasts Errors (RMSFE) in basis points across maturities and forecast horizons. We consider rolling-window estimation with a 240-month window and an initial sample from September 1981 to Augustus 2001 (240 observations) resulting in 230 one-month-ahead forecasts, 225 six-month-ahead forecasts, 219 one-year-ahead forecasts and 207 two-year-ahead forecasts to compute the RMSFEs. The shadow-rate models are all estimated with a fixed lower bound specification of $r_{LB} = 0\%$, while the smooth shadow-rate model has a fixed smoothness parameter $\gamma = 1$. The bold numbers indicate the lowest RMSFE for that particular maturity and horizon.

G.2 Additional CSSFE plots

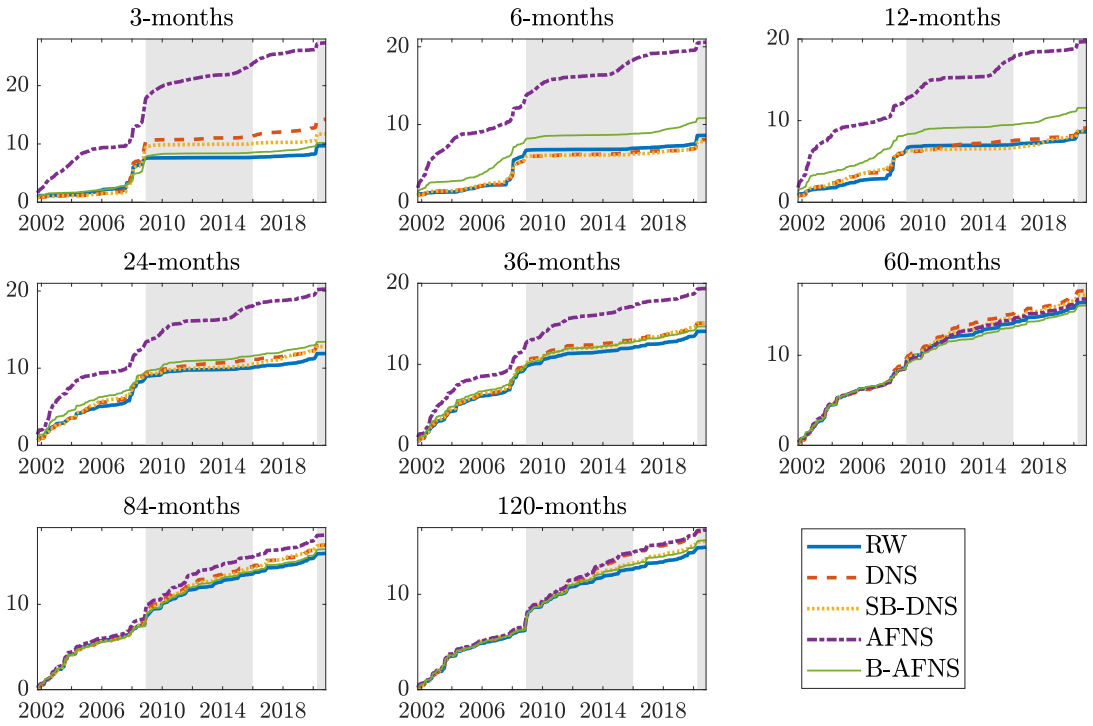

Figure G.1: Cumulative sum of squared forecast errors for one-month ahead forecasts

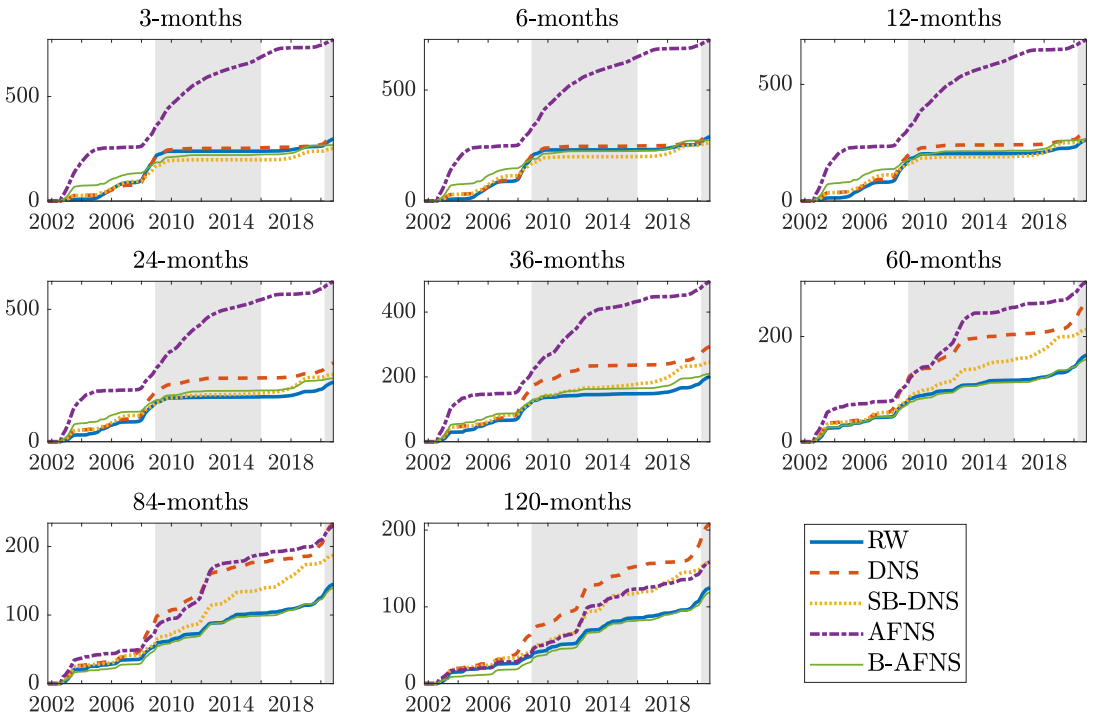

Figure G.2: Cumulative sum of squared forecast errors for one-year ahead forecasts

G.3 Forecasting results for subperiods

Table G.2: Forecasting performance over the pre-ZLB period (September 2001 - October 2008)

	Maturities (in months)							
	3	**6**	**12**	**24**	**36**	**60**	**84**	**120**
Panel A: One-month-ahead forecasts (h = 1)								
RW	29.3	27.3	27.0	**31.6**	**33.2**	31.7	29.6	**26.9**
DNS	33.5	25.8	26.8	32.6	34.1	32.2	30.2	27.4
DNS-TVL	33.5	26.6	25.8	31.9	34.3	32.1	30.3	27.4
SB-DNS	31.7	**25.7**	26.9	32.4	33.7	31.7	29.7	27.2
SB-DNS-TVL	33.1	26.4	**25.8**	31.9	34.2	32.0	30.2	27.3
AFNS	43.9	39.3	38.2	38.9	37.6	31.4	31.1	27.6
B-AFNS	**28.7**	30.3	31.0	33.1	33.6	**31.4**	**29.5**	27.0
Panel B: Six-month-ahead forecasts (h = 6)								
RW	90.4	89.4	85.9	**86.2**	**85.1**	73.1	64.3	55.3
DNS	87.4	89.3	91.5	96.2	94.8	82.7	73.1	63.1
DNS-TVL	84.0	**82.5**	**82.8**	88.0	90.1	81.4	74.0	65.6
SB-DNS	**80.4**	85.5	87.2	89.4	86.7	74.1	64.6	55.9
SB-DNS-TVL	84.0	83.5	84.3	90.1	91.8	82.5	74.6	65.9
AFNS	144.3	139.0	133.4	123.7	110.9	82.0	70.0	53.6
B-AFNS	94.5	99.9	97.9	94.4	88.2	**70.5**	**59.6**	**48.9**
Panel C: One-year-ahead forecasts (h = 12)								
RW	162.4	158.7	148.7	136.7	126.0	100.4	84.7	68.5
DNS	163.0	162.8	159.9	156.0	147.4	123.7	108.3	92.1
DNS-TVL	**140.0**	**137.4**	**134.9**	**134.4**	131.5	115.4	104.7	92.6
SB-DNS	144.9	148.1	144.2	136.5	**125.9**	101.9	87.0	73.7
SB-DNS-TVL	143.9	142.6	140.5	140.5	136.6	118.3	106.1	92.3
AFNS	212.8	206.1	200.5	187.2	166.3	120.6	98.3	71.2
B-AFNS	154.8	157.6	152.6	143.1	128.9	**96.7**	**79.5**	**60.7**
Panel D: Two-year-ahead forecasts (h = 24)								
RW	242.4	239.9	223.1	195.3	169.2	120.2	92.4	**65.0**
DNS	235.9	233.7	220.4	197.2	176.9	142.3	125.0	106.6
DNS-TVL	**184.2**	**180.3**	**171.7**	**160.1**	151.3	131.9	122.6	110.4
SB-DNS	213.4	214.0	198.2	167.4	**141.6**	**103.8**	**86.4**	72.6
SB-DNS-TVL	196.8	193.9	185.6	173.7	163.8	141.7	129.7	114.9
AFNS	251.4	240.0	230.0	207.4	178.7	121.6	93.8	65.5
B-AFNS	231.2	229.5	214.8	187.2	160.5	114.1	89.4	68.2

Notes: This table contains the Root Mean Squared Forecasts Errors (RMSFE) in basis points across maturities and forecast horizons over the pre-ZLB period from September 2001 to October 2008. The shadow-rate models are all estimated with a fixed lower bound specification of $r_{LB} = 0\%$, while the smooth shadow-rate model has a fixed smoothness parameter $\gamma = 1$. The bold numbers indicate the lowest RMSFE for that particular maturity and horizon.

Table G.3: Forecasting performance over the ZLB period (November 2008 - December 2015)

	Maturities (in months)							
	3	**6**	**12**	**24**	**36**	**60**	**84**	**120**
Panel A: One-month-ahead forecasts (h = 1)								
RW	**6.3**	**7.7**	9.7	**13.2**	**17.3**	23.9	**26.5**	**27.3**
DNS	14.1	9.2	12.6	15.0	18.6	25.6	27.6	30.0
DNS-TVL	16.0	10.4	9.6	15.0	20.9	25.8	28.0	29.1
SB-DNS	12.9	7.9	**7.2**	13.4	19.0	25.4	28.0	28.3
SB-DNS-TVL	15.4	10.7	9.6	14.5	19.6	24.6	27.4	27.7
AFNS	29.0	24.1	24.5	24.1	24.0	25.1	29.0	30.1
B-AFNS	13.0	10.2	11.9	15.8	18.6	**23.2**	27.2	28.2
Panel B: Six-month-ahead forecasts (h = 6)								
RW	**37.2**	**39.3**	**40.5**	**43.1**	**49.0**	**61.3**	**65.4**	65.8
DNS	52.3	47.2	45.4	51.8	61.8	73.2	74.9	75.8
DNS-TVL	74.8	70.8	71.0	75.3	81.1	85.4	83.9	82.3
SB-DNS	46.3	42.2	41.4	49.7	60.7	72.7	74.6	73.0
SB-DNS-TVL	68.3	65.0	64.2	66.0	69.6	72.6	71.2	68.1
AFNS	126.0	120.2	116.5	108.7	100.5	86.1	81.7	74.4
B-AFNS	54.8	52.1	52.5	54.8	57.1	61.8	66.0	**65.4**
Panel C: One-year-ahead forecasts (h = 12)								
RW	68.9	70.0	66.5	**58.4**	**58.2**	**69.3**	**75.4**	**76.6**
DNS	80.2	75.8	76.0	82.5	92.5	101.9	102.0	101.7
DNS-TVL	126.9	123.9	125.0	126.5	128.9	126.2	119.6	115.1
SB-DNS	**68.1**	**64.4**	**64.1**	71.3	83.3	95.7	97.2	94.9
SB-DNS-TVL	111.0	107.7	106.7	103.8	102.9	97.7	91.1	86.5
AFNS	201.6	196.3	192.1	178.5	162.0	130.5	115.9	99.5
B-AFNS	70.8	68.8	69.4	68.4	68.5	70.6	77.5	79.5
Panel D: Two-year-ahead forecasts (h = 24)								
RW	184.9	184.6	174.3	152.6	**140.8**	**129.1**	**119.0**	107.4
DNS	216.5	212.3	210.8	209.0	207.6	196.1	179.3	162.4
DNS-TVL	239.5	236.2	236.4	234.3	231.0	215.1	196.0	179.9
SB-DNS	**152.6**	**148.0**	**145.9**	**147.3**	153.0	153.8	143.6	129.1
SB-DNS-TVL	212.4	208.9	207.8	203.7	198.9	181.9	162.5	145.5
AFNS	320.1	315.3	309.9	287.7	258.4	200.4	164.5	125.2
B-AFNS	158.2	155.6	155.6	152.6	146.6	131.6	122.6	**107.2**

Notes: This table contains the Root Mean Squared Forecasts Errors (RMSFE) in basis points across maturities and forecast horizons over the ZLB period from November 2008 to December 2015. The shadow-rate models are all estimated with a fixed lower bound specification of $r_{LB} = 0\%$, while the smooth shadow-rate model has a fixed smoothness parameter $\gamma = 1$. The bold numbers indicate the lowest RMSFE for that particular maturity and horizon.

Table G.4: Forecasting performance over the most recent period (January 2016 - October 2020)

	Maturities (in months)							
	3	**6**	**12**	**24**	**36**	**60**	**84**	**120**
Panel A: One-month-ahead forecasts (h = 1)								
RW	18.5	16.9	16.4	17.7	18.7	20.0	**20.5**	**20.1**
DNS	22.1	16.7	16.4	18.0	18.9	21.2	21.0	20.8
DNS-TVL	20.8	16.2	**15.9**	**17.4**	**18.4**	20.5	21.0	20.7
SB-DNS	**16.7**	16.6	19.0	19.8	19.6	20.8	21.2	20.1
SB-DNS-TVL	17.8	**15.6**	16.8	18.3	19.1	21.0	21.4	21.2
AFNS	24.7	20.0	18.5	19.5	19.6	**20.0**	21.1	20.5
B-AFNS	16.8	18.6	19.0	17.9	18.4	20.5	21.3	21.1
Panel B: Six-month-ahead forecasts (h = 6)								
RW	62.0	61.7	61.5	61.7	62.4	61.2	59.2	57.3
DNS	63.9	59.5	59.2	62.1	64.1	66.3	64.4	63.3
DNS-TVL	57.9	53.8	**53.8**	**57.0**	59.7	62.9	62.2	61.4
SB-DNS	55.3	60.7	66.3	68.1	66.9	64.0	61.0	55.8
SB-DNS-TVL	**51.1**	**52.5**	56.1	60.0	62.2	64.8	64.1	63.5
AFNS	80.1	74.7	72.0	71.2	68.9	63.7	60.9	**55.6**
B-AFNS	60.4	61.5	60.3	58.3	**58.8**	**60.0**	**58.9**	56.4
Panel C: One-year-ahead forecasts (h = 12)								
RW	100.4	101.0	101.1	97.9	95.9	90.9	85.6	82.4
DNS	93.9	93.1	95.7	98.6	99.8	100.9	98.6	98.3
DNS-TVL	81.8	**80.9**	**84.2**	**88.8**	91.3	93.5	91.8	90.8
SB-DNS	96.3	103.4	109.7	110.5	107.2	98.9	91.8	82.2
SB-DNS-TVL	**80.8**	85.2	90.8	94.4	95.6	96.8	95.2	94.5
AFNS	119.9	115.2	112.8	108.9	103.0	91.8	85.3	**77.7**
B-AFNS	88.1	90.5	91.2	89.2	**88.5**	**86.9**	**83.7**	79.7
Panel D: Two-year-ahead forecasts (h = 24)								
RW	127.4	130.2	134.0	131.3	128.1	121.7	115.1	110.5
DNS	120.7	123.7	128.3	131.4	133.3	136.7	137.2	141.4
DNS-TVL	**106.6**	**108.5**	**112.9**	**116.7**	**118.8**	121.0	120.0	122.0
SB-DNS	138.8	146.0	152.3	154.9	154.0	144.5	133.5	118.1
SB-DNS-TVL	115.2	120.4	124.8	125.1	123.8	121.8	119.5	119.8
AFNS	169.8	164.6	160.0	151.6	141.8	124.2	**114.2**	**105.3**
B-AFNS	127.2	130.8	132.3	129.3	126.7	**120.9**	114.6	108.2

Notes: This table contains the Root Mean Squared Forecasts Errors (RMSFE) in basis points across maturities and forecast horizons over the most recent period from January 2016 to October 2020. The shadow-rate models are all estimated with a fixed lower bound specification of $r_{LB} = 0\%$, while the smooth shadow-rate model has a fixed smoothness parameter $\gamma = 1$. The bold numbers indicate the lowest RMSFE for that particular maturity and horizon.

References

Black, F. (1995): "Interest Rates as Options," *The Journal of Finance*, 50, 1371–1376.

Caldeira, J. F., G. V. Moura, A. A. P. Santos, and F. Tourrucôo (2016): "Forecasting the yield curve with the arbitrage-free dynamic Nelson–Siegel model: Brazilian evidence," *EconomiA*, 17, 221–237.

Christensen, J. H., F. X. Diebold, and G. D. Rudebusch (2011): "The affine arbitrage-free class of Nelson–Siegel term structure models," *Journal of Econometrics*, 164, 4–20.

Christensen, J. H. E. and G. D. Rudebusch (2015): "Estimating Shadow-Rate Term Structure Models with Near-Zero Yields," *Journal of Financial Econometrics*, 13, 226–259.

Duffee, G. R. (2002): "Term Premia and Interest Rate Forecasts in Affine Models," *The Journal of Finance*, 57, 405–443.

Duffie, D. and R. Kan (1996): "A Yield-Factor Model of Interest Rates," *Mathematical Finance*, 6, 379–406.

Durbin, J. and S. J. Koopman (2012): *Time Series Analysis by State Space Methods*, Oxford University Press, 2 ed.

Fisher, M. and C. Gilles (1996): "Term premia in exponential-affine models of the term structure," Manuscript, Board of Governors of the Federal Reserve System.

Hamilton, J. D. (1994): "State-space models," in *Handbook of Econometrics*, Elsevier, vol. 4, 3039–3080.

Krippner, L. (2012): "Modifying Gaussian term structure models when interest rates are near the zero lower bound," *CAMA Working Papers*, 48.

——— (2015): *Zero Lower Bound Term Structure Modeling: A Practioners Guide*, Palgrave Macmillan.

Nelson, C. R. and A. F. Siegel (1987): "Parsimonious Modeling of Yield Curves," *The Journal of Business*, 60, 473–489.